ON PRETZEL KNOTS AND CONJECTURE $\mathbb{Z}$

JESÚS RODRÍGUEZ VIORATO AND FRANCISCO GONZALÉZ ACUÑA

Abstract. Conjecture $\mathbb{Z}$ is a knot theoretical equivalent form of the Kervaire Conjecture. We show that Conjecture $\mathbb{Z}$ is true for all the pretzel knots of the form $P(p, q, -r)$ where p, q and r are odd positive integers.

1. Introduction

A well known unsolved conjecture in combinatorial group theory is the so called Kervaire Conjecture.

Conjecture 1.1 (Kervaire Conjecture)**.** *Let G be a group, $G \neq 1$. Then $\mathbb{Z} * G$ cannot be normally generated by one element.*

F. González-Acuña and A. Ramírez in [**?**] have stated a knot theoretical conjecture equivalent to the Kervaire Conjecture, which they call Conjecture $\mathbb{Z}$.

Conjecture 1.2 (Conjecture $\mathbb{Z}$)**.** *If F is a compact orientable and non-separating surface properly embedded in a knot exterior E, then $\pi_1(E/F) \approx \mathbb{Z}$.*

They were able to prove that when ∂F is connected, $\pi_1(E/F) \approx \mathbb{Z}$ (See Proposition 11 in [**?**]).

We will say that a surface F in a knot exterior E has Property $\mathbb{Z}$ if $\pi_1(E/F) \approx \mathbb{Z}$. And we will say that a knot k has Property $\mathbb{Z}$ if for every compact orientable and non-separating surface (CON surface) F in E (the exterior of k) it is true that $\pi_1(E/F) \approx \mathbb{Z}$.

By Lemma 5.1 we may assume, without loss of generality, that F is incompressible. That is, if we were able to prove that every incompressible, compact, orientable and non-separating surface (ICON surface) F in the exterior E of a knot K has Property $\mathbb{Z}$, then it would follow that the knot K has Property $\mathbb{Z}$ too. This is why ICON surfaces are important.

Now, it is natural to ask if there are ICON surfaces with disconnected boundary. M. Eudave-Muñoz answered this question in [**?**]. In fact, for every odd number n, he found a family of ICON surfaces with exactly n components on their boundary. He also proved that those surfaces have Property $\mathbb{Z}$. But it is still unknown if the corresponding knots of those surfaces have Property $\mathbb{Z}$.

The next question that arises is that if there are knots that have Property $\mathbb{Z}$. F. González-Acuña and A. Ramírez in [**?**] noted the existence of two families:

- The fibered knots have Property $\mathbb{Z}$. This is because $\pi_1(E)$ has as a quotient $\pi_1(E/F) \cong \mathbb{Z} * P$ where P is a perfect group. Proving by contrapositive, if P is not trivial then the commutator subgroup of $\mathbb{Z} * P$ is not finitely generated, implying that the commutator subgroup of $\pi_1(E)$ also is not finitely generated, which means that E can't be the exterior of a fiber knot.

- A knot K has Property $\mathbb{Z}$ if the fundamental group of its exterior has rank two. This is because rank two implies that $\mathbb{Z} * P$ has rank at most two and so, by [**?** , Chapter 4, Corollary 1.9], the perfect group P has rank at most 1 and is therefore trivial.

Now, we are interested in finding another family of knots having Property $\mathbb{Z}$. The family that immediately came to our mind was the Montesinos knots family; because we can make use of the classification of incompressible surfaces that A. Hatcher and U. Oertel made in [**?**].

We were able to find ICON surfaces in Montesinos knots exteriors; moreover, we were able to classify the ICON surfaces in the family of pretzel knots $P(p, q, -r)$ where p, q and r are positive odd numbers (see Theorem 4.9). In this family of knots there exist examples of ICON surfaces where the number of boundary components is an arbitrary odd positive number.

We also were able to prove that all those pretzels ($P(p, q, -r)$ where p, q and r are positive odd numbers) have Property $\mathbb{Z}$ (see Theorem 5.4).

None of these pretzel knots is a fiber knot (see M. Hirasawa and K. Murasugi in [**?**]) when p, q and r are grater then one. And, by the results of E. Klimenko and M. Sakuma in [**?**], neither of these knots is of rank two except possibly for the pretzels $P(3, 3, -r)$ with $r \not\equiv 0 \pmod 3$; and only $P(3, 3, -1)$ has tunnel number one. Then, this is a new family of knots having Property $\mathbb{Z}$.

2. Preliminaries

In this first section, we are going to describe the work of A.E. Hatcher and U.Oertel in [**?**]. And later, we are going to add some modifications to be able to determine orientability and connectedness of the surfaces constructed.

2.1. **Train tracks.** First, we are going to recall the topological version of train track developed by A.E. Hatcher in [**?**]. We are going to extend that concept in 3.1. In order to do this, first we are going to separate the concept of train track into two parts; diagram and weights.

Definition 2.1. A *train track diagram* T in a surface F, is a graph that satisfies the following conditions:

(1) T only has vertices of degree one or three.
(2) T is properly embedded in F. This means that $\partial F \cap T$ is the set of degree one vertices of T.
(3) All vertices of degree three are locally diffeomorphic to the next picture:

To complete the definition of train track, what we need is to put weights on the edges of the train track diagram.

Definition 2.2. Let T be a train track diagram. We say that a function $f : \text{edges}(T) \to \mathbb{Z}^+$ assigns weights compatible with T if $f(c) = f(a) + f(b)$ for all the triplets of edges a, b and c around a vertex of degree three, in the same order as in Fig. 2.

With the latest two concepts, we can now easily write the definition of train track.

Definition 2.3. A *train track* in a surface F is a train track diagram T in F with an assignment of weights compatible with T.

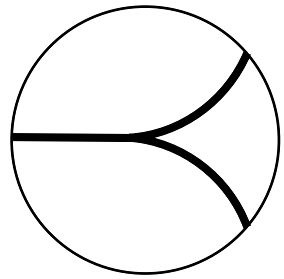

FIGURE 1. Vertices of degree three in a train track diagram

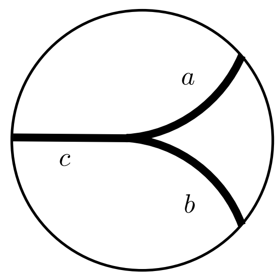

FIGURE 2. Weights around a vertex of degree three

The weights allow us to build a *curve system* (a set of disjoint arcs and curves properly embedded) in the surface F. This can be done as follows:

- For each edge of T, take as many parallel copies as its assigned weight.
- On degree three edges, one of the edges has assigned weight equal to the sum of the other two. So, it is possible to join the endpoints of the first edge with the others, in a natural way.

Figure 3 shows an example of this construction on an edge with weights 5, 3 and 2.

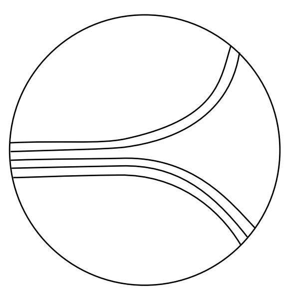

FIGURE 3. Local view of a vertex of degree three

2.2. **Incompressible surfaces on Montesions knots.** We are now going to describe the work of A. Hatcher and U. Oertel in [**?**] where they classify the incompressible surface in the exterior of Montesinos knots. We also present some notation and explain the relation with the train tracks.

We are going to consider S^3 as the join of two circles A and B; let the circle B be subdivided as an n-sided polygon. Then the join of A with the ith edge of B is a ball B_i. These n balls B_i cover S^3, meeting each other only in their boundary spheres. The circle $A \subset S^3$, called the *axis*, is the intersection of all the B_is (see Fig. 4).

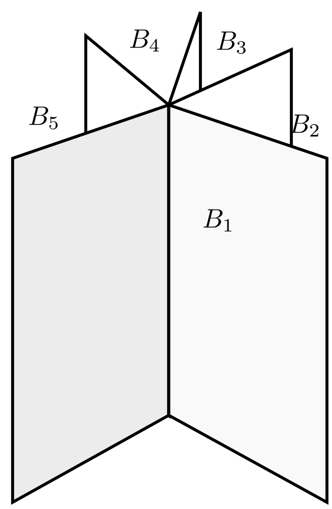

FIGURE 4. Decomposition of S^3 as the union of $n = 5$ 3-balls

Inside any ball B_i, K looks like Fig. 5. That is, $K_i = K \cap B_i$ is a rational tangle of slope p_i/q_i on B_i and $K_i = K_i' \cup K_i''$ where $K_i' = \{\text{four point}\} \times [0, 1]$ contained in a collar neighborhood $S^2 \times [0, 1]$ of ∂B_i and K_i'' is the union of two disjoint arcs on $S^2 \times \{0\} \subset \text{int}(B_i)$. We denote $K = M(p_1/q_1, \ldots, p_n/q_n)$.

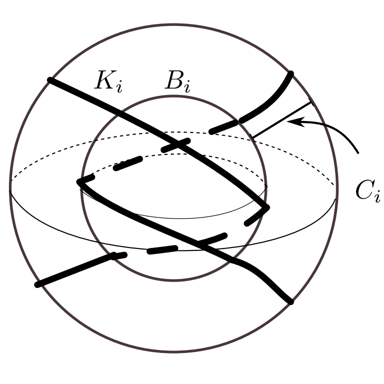

FIGURE 5. Montesinos knots inside B_i.

Now, let F be an incompressible and ∂-incompressible surface properly embedded in $E = S^3 - \nu(K)$, where K is a Montesinos knot and $\nu(K)$ is the open regular neighborhood of K. We are interested in the case when $\partial F \neq \emptyset$, so we are going to add that condition.

Move F until ∂F is transversal to all small meridians of K and intersect them in the same number of points. Denote with m the number of points that ∂F intersects each meridian; we will call m the *number of sheets* of F.

Isotope again F but now to be transversal to the axis of the Montesinos knot K and reduce the number of points in the intersection to the minimum possible.

Now, move F to put ∂F outside of S_i^0 $(= S^2 \times \{0\} \subset B_i)$. So, the intersection $F \cap S_i^0$ can be reduced to a (possible empty) disjoint collection of parallel loops that are boundary of parallel circles which separate the arcs of the rational tangle (we will refer to these parallel loops as *slope* p_i/q_i *loops*).

How this reduction is done, is explained in [**?**]. So, F inside S_i^0 is a (possible empty) disjoint union of slope p_i/q_i loops and, the rest of F lies inside a collar C_i of ∂B_i.

Finally, put F so that the restriction to F of the natural projection of C_i on to $[0, 1]$ is a Morse function.

We will now study how F intersects any of the levels of the Morse function, that is, study the intersection of F with $\partial B_i \times \{t\} - \nu(K)$ for each value $t \in [0, 1]$. The sphere with four holes $\partial B_i \times \{t\} - \nu(K)$ will be denoted by S_i^t.

Observe that $S_i^t \cap F$ is, for almost all values of t, a system of disjoint arcs and curves properly embedded in S_i^t, except for a finite number of values $t_0, t_1, \ldots$ where F has a saddle and $S_i^t \cap F$ has a singularity.

Each curve system $S_i^t \cap F$ can be represented by a train track and if F is oriented, then we can orient the train track. Because the number of arcs incident to each hole is the same, the possible train tracks diagrams that we can get for this type of curve systems are the ones shown on figure 6 (see [**?**]).

2.3. **The edgepath system model.** When passing through a saddle point, a train track can only transform into a certain set of train tracks (depending on its diagram and mostly on its assigned weights). With this in mind, Hatcher and Oertel created a diagram $\mathscr{D} \subset \mathbb{R}^2$ where any two train tracks connected by a saddle are located as two nearby points.

In this diagram, any train track is represented as a point on the diagram. Moreover, a train track and any of its multiples is represented by the same point. Here, a train track is a "multiple" of one another if all its weights are obtained by a multiplication by a constant from the weights of the other.

Let us start by defining the diagram $\mathscr{D}$ as a set in $\mathbb{R}^2$ that contains all the points $(1 - 1/n, m/n)$ and $(1, m/n)$ with $n \in \mathbb{Z}^+$, $m \in \mathbb{Z}$ and $(m, n) = 1$. We will use the following notation for those points: $\langle m/n \rangle = (1 - 1/n, m/n)$ and $\langle m/n \rangle_0 = (1, m/n)$.

Then, we add the segments joining $\langle m_1/n_1 \rangle$ with $\langle m_2/n_2 \rangle$ when $m_1 n_2 - m_2 n_1 = \pm 1$. Those segments are denoted by $\langle m_1/n_1, m_2/n_2 \rangle$.

Also we add the horizontal segments joining $\langle m/n \rangle$ with $\langle m/n \rangle_0$. We almost got the full diagram $\mathscr{D}$; it remains only to add the point $\langle \infty \rangle = (-1, 0)$ and the segments $\langle \infty, n/1 \rangle$ with $n \in \mathbb{Z}$.

We will call edges to the segments $\langle \alpha, \beta \rangle$ of $\mathscr{D}$. Fig. 7 shows how diagram $\mathscr{D}$ looks like.

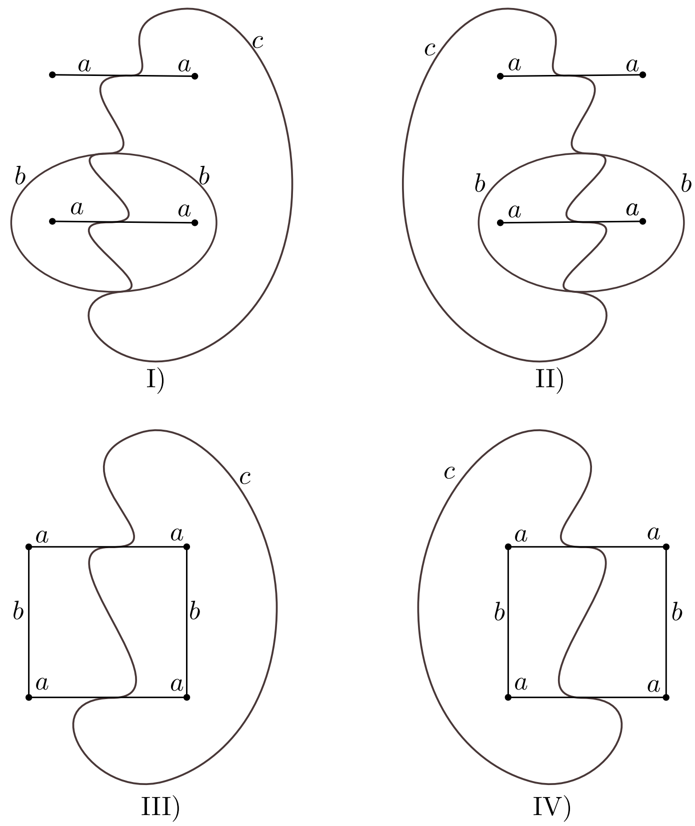

FIGURE 6. Train tracks diagrams that determine all the essential curve systems on a sphere with four holes.

When we remove the set $\mathscr{D}$ from $\mathbb{R}^2$ what remains are planar regions, some of them are triangular. We will call these triangular regions triangles of $\mathscr{D}$ and we will add them to $\mathscr{D}$. So, now we can think of $\mathscr{D}$ as a 2-dimensional simplicial complex.

As we said before, we will associate train tracks to points on $\mathscr{D}$. For each train track with one of the diagrams of Fig. 6, we associate a point of $\mathscr{D}$ with the following rules:

- If the train track has a diagram of type I with weights (a, b, c), we associate the point $(\frac{b}{a+b}, \frac{c}{a+b})$.
- If the train track has a diagram of type II with weights (a, b, c), we associate the point $(\frac{b}{a+b}, -\frac{c}{a+b})$. In this case we will say that the diagram is of type I but with weights $(a, b, -c)$.
- If the train track has a diagram of type III with weights (a, b, c), we associate the point $(-\frac{b}{a+b}, \frac{c}{a+b})$.
- If the train track has a diagram of type IV with weights (a, b, c), we associate the point $(-\frac{b}{a+b}, -\frac{c}{a+b})$. In this case we will say that the diagram is of type III but with weights $(a, b, -c)$.

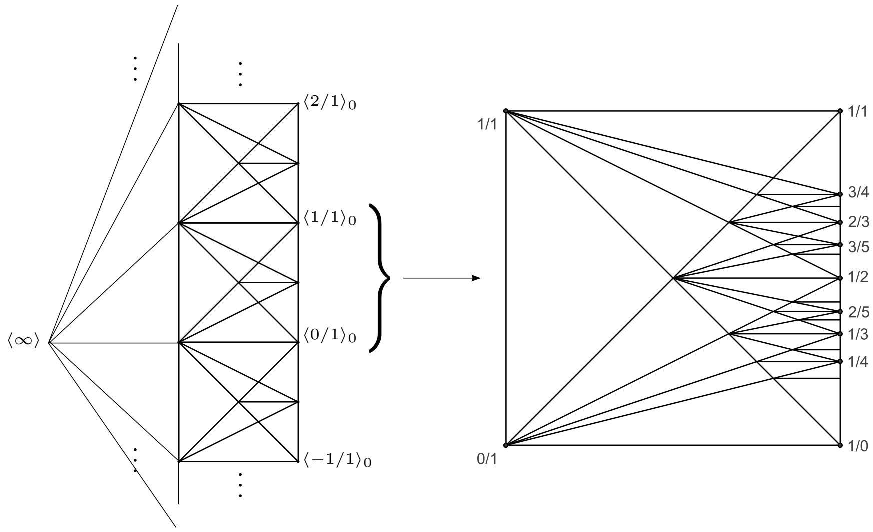

FIGURE 7. Diagram $\mathscr{D}$

This assignment of triples to points on $\mathscr{D}$ may seem artificial, but will make sense when we study its properties. First of all, let us observe that it is a "projective relation", that is, a train track and its multiples are assigned to the same point. And when two train tracks are assigned to the same point, then one is a multiple of the other.

Another property is that a pair of arcs with slope p/q (p possibly negative), in the sphere with four holes, can be obtained by a train track diagram of type I or II with weights $(1, q-1, p)$; then they correspond to the point $\langle p/q\rangle$. The same happens with slope p/q loops; they correspond to the point $\langle p/q\rangle_0$.

Also, two pairs of arcs of slopes p/q and r/s (respectively) can be placed over the same sphere with four holes without any intersection if and only if $ps - qr = \pm 1$. And when this happens, we can take α parallel copies of the pair of arcs of slope p/q and β parallel copies of the other, where α and β are any positive integers. The system of curves thus constructed is associated to a point on the segment $\langle p/q, r/s\rangle$ in $\mathscr{D}$ with the following coordinates:

$$\left(1 - \frac{\alpha+\beta}{\alpha q + \beta s}\ ,\ \frac{\alpha p + \beta r}{\alpha q + \beta s}\right) \in \langle p/q, r/s\rangle$$

We will denote such point as $\alpha'\langle p/q\rangle + \beta'\langle r/s\rangle$, where $\alpha' = \alpha/(\alpha+\beta)$ and $\beta' = \beta/(\alpha+\beta)$. This notation is self explained by the projectivization property of $\mathscr{D}$.

Finally, something similar happens to a set of three disjoint pairs of arcs, but that will not be necessary in this paper.

The part of $\mathscr{D}$ contained in the half-plane $x \geq 0$ will be an infinite strip $\mathscr{S}$. Most of the time, we are going to work on $\mathscr{S}$. On the other hand, there is an extra edge of $\mathscr{D}$, the segment that joins $\langle\infty\rangle_0 = (-2, 0)$ with $\langle\infty\rangle$. When we add this extra edge, we will call $\hat{\mathscr{D}}$ the extension of $\mathscr{D}$.

2.4. **Candidate surfaces.** An edgepath in the diagram $\mathscr{D}$ is a path contained in the 1-skeleton of $\mathscr{D}$.

Definition 2.4. For a Montesions knot $K = M(p_1/q_1, p_2/q_2, \ldots, p_n/q_n)$, let edgepaths γ_i in $\mathscr{D}$ be given, $i = 1, \ldots, n$ with the following properties:

- (E1) The starting point of γ_i lies on the edge $\langle p_i/q_i, p_i/q_i\rangle$, and if the starting point is not the vertex $\langle p_i/q_i\rangle$, then the edgepath γ_i is constant.
- (E2) γ_i is *minimal*, i.e., it never stops and retraces itself, nor does it ever go along two sides of the same triangle of $\mathscr{D}$ in succession.
- (E3) The ending points of the γ_i's are rational points of $\mathscr{D}$ which all lie on one vertical line and whose vertical coordinates add up to zero.
- (E4) γ_i proceeds monotonically from right to left, "monotonically" in the weak sense that motion along vertical edges is permitted.

We are going to associate a family of surfaces to these n edgepaths that satisfy the conditions E1-E4. But first let us look at a couple of definitions.

Any edgepath γ_i ends at a point of rational coordinates on a segment of $\mathscr{D}$; let us say a point on $\langle p/q, r/s\rangle$. Then this point can be written uniquely as:

$$\alpha \langle p/q\rangle + \beta \langle r/s\rangle$$

with $\alpha, \beta \in \mathbf{Q}^+$ and $\alpha+\beta = 1$. We will call β the fraction of the edge traveled by γ_i at the last edge. Denote by $\langle p/q\rangle \to \alpha\langle p/q\rangle + \beta\langle r/s\rangle$ to indicate that an edgepath went first from $\langle p/q\rangle$ and then advanced in direction of $\langle r/s\rangle$ but only a fraction β.

Finally, we will call *length of a path* γ_i to the number of complete edges that are traveled by γ_i plus the fraction of edge at the last edge. Denote this number by $|\gamma_i|$. So, $|\gamma_i| = 0$ if and only if γ_i is the constant path.

To construct a surface from a given edgepath system that satisfies conditions E1-E4 first we have to choose a positive integer m such that for any i, the train track associated with the end points of γ_i can be scaled to have weight m at the four vertices. This m can be any common multiple of all a_i's, where (a_i, b_i, c_i) is a triplet associated to the final point of γ_i (when the endpoints have negative x-coordinate m is common multiple of $a_i + b_i$).

By its definition, the number m will correspond to the number of leaves of the surfaces we are going to construct.

Now, to each edgepath γ_i we are going to associate a finite set of 2-manifolds F_i in B_i such that $\partial F_i \subset K_i \cup \partial B_i$ and such that meridians of K_i intersect F_i in exactly m points.

If the path γ_i is constant, then the starting point is on $\langle p_i/q_i, p_i/q_i\rangle_0$ and is associated with a unique system of arcs and curves in B_i^0; such a system consists of m parallel copies of the pair of arcs with slope p_i/q_i and many other parallel copies of slope p_i/q_i loops; the number of parallel copies of the loops depends on the location of the starting point in the segment $\langle p_i/q_i, p_i/q_i\rangle_0$. Then, F_i would be the product of the curve system with an interval, which is contained in the collar $C_i \subset B_i$, together with a disjoint union of disk capping off the slope p_i/q_i loops on $\partial B_i \times 0$.

When γ_i it is not constant, we are going to construct F_i in the collar $\partial B_i \times [0, 1]$ by describing the sequence of saddle points of the Morse function given by the projection to $[0, 1]$. Let start with m parallel copies of a pair of arcs of slope p_i/q_i at $t = 0$, for each edge $\langle r_0/s_0, r_1/s_1\rangle$ of γ_i we will add m saddle points to change

m parallel arcs of slope r_0/s_0 to m arcs of slope r_1/s_1. Each saddle can be chosen in two different ways as in Fig. 8.

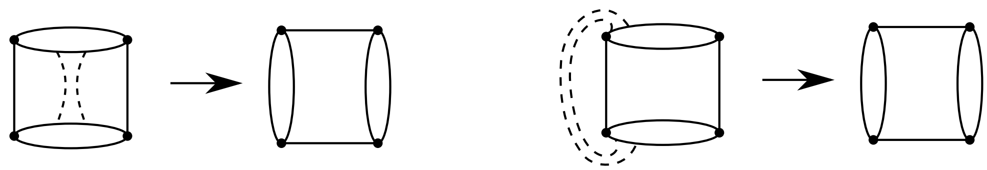

FIGURE 8. Saddles can be chosen in two different ways

Once the γ_i and m are chosen, we only have a finite number of possibilities of F_i.

From condition E3 all F_i will fit together to form a 2-manifold F, called a *candidate surface*[1]. To illustrate how this is done, let us start by gluing F_1 and F_2.

Suppose that the train track that describes the system of curves of ∂F_i in ∂B_i is the one shown on Fig. 6 I, and recall that the a-coordinate on their triplet of weights is the same, that is, the triplet of weights have the form (a, b_1, c_1) and (a, b_2, c_2). But, the condition E3 says that all x-coordinates on $\mathscr{D}$ are the same, this translates onto $b_1/(a+b_1) = b_2/(a+b_2)$; then $b_1 = b_2$ $(= b)$.

The axis of the knot divides each pair $(\partial B_i, \partial F_i)$ into two isomorphic pairs of disks and arcs. Having both a and b coordinates equal, any pair on ∂B_1 can be identified isomorphically with any pair on ∂B_2. For instance, on Fig. 9, we can identify the right disc on a) with the left disk of b).

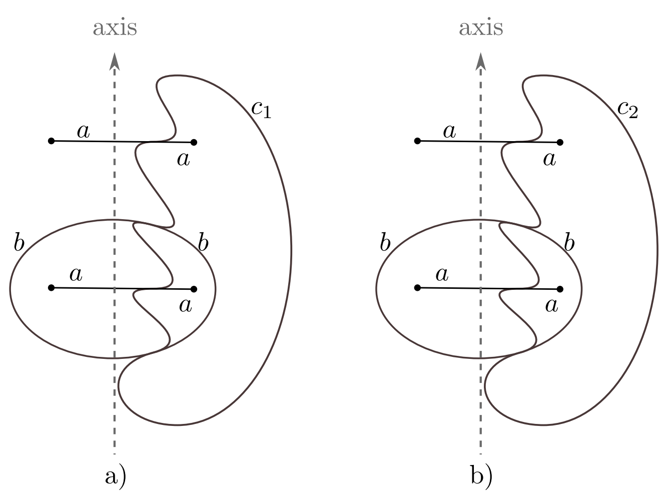

FIGURE 9. Train tracks on the boundary of B_1 and B_2

[1]Hatcher and Oertel use "surface" as a synonymous of 2-manifold. So candidate surfaces could be disconnected 2-manifolds. But in any other context, we are going to use surface as a connected 2-manifold.

It would be easier to identify these disks if we make a little twist around the axis on the ball B_2, such that, the left disk looks exactly as a reflection of the right disk of B_1 (see Fig. 10).Notice, that after this twist the value of c on the right disk of B_2 will be c_1+c_2. If we glue now B_3, and so on, at the end we will have to glue B_n with B_1 to close the cycle, but this will be only possible if $c_1+c_2+\cdots+c_n=0$; this is equivalent to saying that all the y-coordinates of the edge path add up to zero, i.e, condition E3. See Fig. 27 and Fig. 28 for another example.

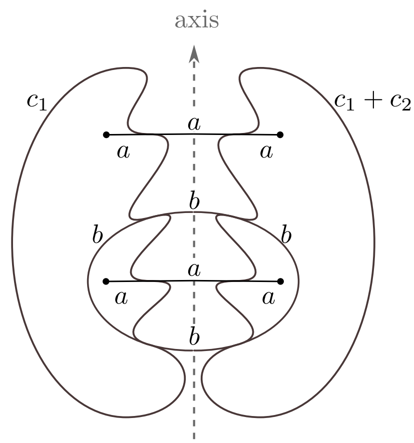

FIGURE 10. Train track of type I with weights (a, b, c_2) after twisting $c_1/(a+b)$ times around the axis

Moreover, there are some extension of candidate surfaces when the ends of the edgepaths are on the extended diagram $\hat{\mathscr{D}}$; for the full details of the definition of candidate surface see [**?**]. Also in that article they prove the following proposition.

Proposition 2.5 (Hatcher and Oertel)**.** *Every incompressible, ∂-incompressible surface in the exterior of K having non empty boundary of finite slope is isotopic to one of the candidate surfaces.*

2.5. **Computing slope.** Let F be a candidate surface constructed as before, using a set of edgepaths γ_i and a chosen m as the number of sheets. We define the twisting of F as

$$\tau(F)=2(s_- - s_+)/m$$

where s_+ (s_-) is the number of saddles on F that increase (decrease) the slope. Saddles that produce slope ∞ or arcs, do not contribute to the value of $\tau(F)$.

A formula in terms of γ_i's is

$$\tau(F)=2(e_- - e_+)$$

where $e_+(e_-)$ is the number of γ_i's that increase (decrease) the slope, and fractional values of $e_\pm$ corresponding to the final edge are allowed. Similarly, edges connected to $\langle\infty\rangle$ or $\langle\infty\rangle_0$ do not contribute to the value of $\tau(F)$.

And the boundary slope of F is

$$m(F)=\tau(F)-\tau(F_0) \tag{1}$$

where F_0 is a Seifert surface in the knot exterior. Computing $\tau(F_0)$ is possible; we just need to build a set of edgepaths satisfying conditions E1-E4 with $m = 1$ and keeping orientability.

It is convenient to reduce modulo 2 the values p and q in all the vertices $\langle p/q \rangle$ of $\mathscr{D}$. With this reduction, all triangles in $\mathscr{D}$ have three different vertices: $\langle 1/1 \rangle$, $\langle 0/1 \rangle$ and $\langle 1/0 \rangle$. Now, the condition of orientability in F_0 is that each edgepath must use only one type of edge modulo 2 reduction: $\langle 1/1, 0/1 \rangle$, $\langle 0/1, 1/0 \rangle$ or $\langle 1/0, 1/1 \rangle$. We call *monochromatic* to the edgepath that satisfies that condition.

When the pretzel knot has only one even q_i we choose a monochromatic edgepath from $\langle p_i/q_i \rangle$ to $\langle \infty \rangle$ for every i. This edgepath is unique for the odd q_i and for the even q_i there are two monochromatic options, but only one will make the final union orientable. When all the q_i's are odd, we choose monochromatic edgepaths passing for vertices with odd denominator and ending on a vertex at the left border of $\mathscr{S}$; those edgepaths are unique except for some vertical extensions that do not affect the value of $\tau(F_0)$.

2.6. **Finding the edgepath system satisfying E1-E4.** In order to find the edgepaths system, we divide them into three types:

Type I. When all the edgepath ends have positive horizontal coordinates. That is, when all the edgepath ends are inside $\mathscr{S}$. In this case, the set of possible edgepaths is computed using the Euclidean algorithm as the main tool.

Type II. This is when all the edgepath ends are on the left border of $\mathscr{S}$. This system can be extended vertically as much as we want.

Type III. This is when the edgepath ends are on an edge with the $\langle \infty \rangle$ vertex. This particular system of edgepaths can be extended as close to $\langle \infty \rangle$ as we want.

An algorithm is explained in [**?**] which, given $p_1/q_1, \ldots, p_n/q_n$ finds all the edgepath systems, of type I, II and III, satisfying E1-E4.

3. The ICON surfaces

Recall that ICON stands for incompressible, compact, orientable and non-separating surface. So in order to prove that some Montesinos Knots have Property $\mathbb{Z}$, we are going to modify the theory of Hatcher and Oertel to describe orientability and connectedness of their candidate surfaces. That is why we developed the concept of oriented train track.

3.1. **Oriented train track.** Now, instead of using integers as weights, we are going to use elements of the free semigroup of rank two; denoted by $\mathbb{P}_2$. We will represent the elements of $\mathbb{P}_2$ as finite sequences of symbols 1 and -1 and we will denote its concatenation operation as $\oplus$; for example, $(1, -1) \oplus (-1, -1, 1) = (1, -1, -1, -1, 1)$.

Now, let J be the function $J : \mathbb{P}_2 \to \mathbb{P}_2$ such that

$$J(\epsilon_1, \epsilon_2, \ldots, \epsilon_n) = (\epsilon_n, \epsilon_{n-1}, \ldots, \epsilon_1)$$

Remark 3.1. The function J will become very important later on, mostly in the proof of Theorem 4.9.

Let $Edges(T)$ be the set of edges of T with directions, or more precisely,

$$Edges(T) = \{(v_1, v_2) | v_1, v_2 \in \text{vertices}(T) \text{ and } v_1v_2 \text{ an edge of } T\}.$$

In this sense, if $a = (v_1, v_2) \in Edges(T)$ then $a^{-1} = (v_2, v_1)$ is another element of $Edges(T)$.

Definition 3.2. Consider a train track diagram T in an oriented 2-manifold F. A function $f : Edges(T) \to \mathbb{P}_2$ is an *orientation* of T if

(1) $f(a^{-1}) = -J \circ f(a)$ for all $a \in Edges(T)$
(2) For all a, b and c edges with a common vertex, and oriented as shown in Fig. 11 (viewed from the positive side of F), f satisfies:

$$f(c) = (f(a), f(b)) = f(a) \oplus f(b)$$

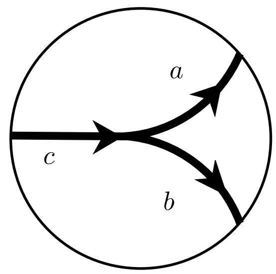

FIGURE 11. Oriented edges around a vertex of degree 3

Consider the function $|\cdot| : \mathbb{P}_2 \to \mathbb{Z}^+$ that assigns to an element its length; for example, $|(1,-1,1)| = 3$. The composition of an orientation f, of a train track diagram, with $|\cdot|$ give us a weight assignation in the usual sense; that is, an oriented train track determines a regular train track. In the other way around, for any train track T we can orientate its arcs in any direction and obtain an oriented train track. In general, there is a finite set of oriented train tracks that can be obtained like this; we denote such set as $\mathcal{O}(T)$.

Using an oriented train track we can construct an oriented disjoint set of arcs and curves. Just take an edge a on T, oriented in any way, consider v_a its corresponding oriented weight. Now, take $|v_a|$ parallel copies of a, and orient them in the same direction or in opposite direction of a if the corresponding entry on v_a is positive or negative, respectively. The correspondence between entries of v_a and the parallel copies of a, is from left to right (view Fig. 12). This construction is independent of the original orientation of a, thanks to the property 1 of Definition 3.2.

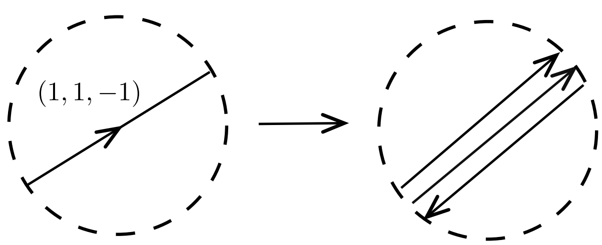

FIGURE 12. An example of parallel copies taken

On a vertex of degree three, we can suppose that the three arcs around it are oriented as in Fig. 11. Then, the copies parallel to c can be well joined with the copies of a and c, so that, we end with a disjoint set of oriented curves and arcs properly embedded in F (see Fig. 13).

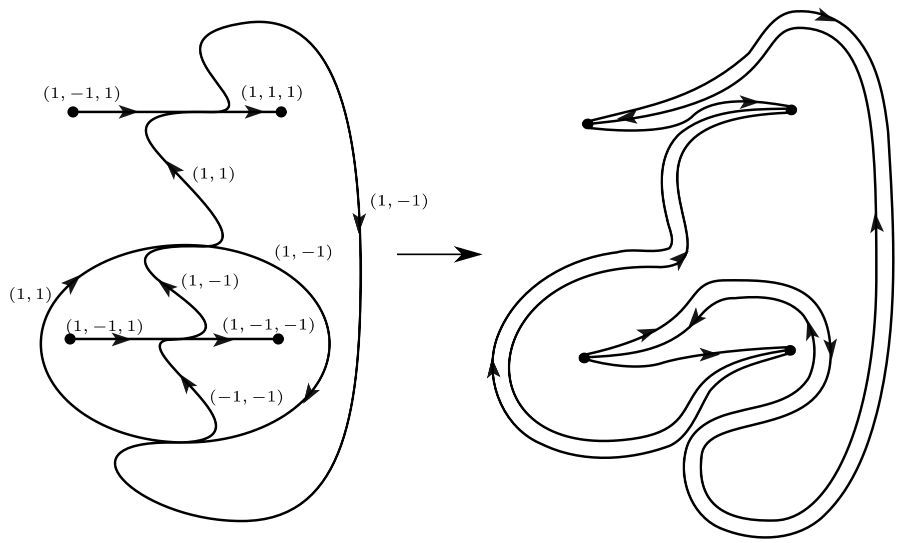

FIGURE 13. Transforming an oriented train track into a disjoint set of oriented curves and arcs

Notice that property 1 implies that the weight of $-a$ is determined by the weight of a. So, in order to orient a train track diagram T we only need to specify the weight for only one orientation of each edge of $a \in T$. In other words, we must orientate all the edges of T on any direction and later specify the weights of those edges. For example, Fig. 13 represents an oriented train track.

Another object that we will require, is a parametrized train track, which we understand as an orientated train track but instead of 1's and -1's, we use variables.

Definition 3.3. A *parametrized oriented train track* with n parameters is a function $\{-1, 1\}^n \to \mathcal{O}(T)$ for some train track T and a positive integer n.

Fig. 14 shows an example of a parametrized oriented train track where $n = 2$. In this example, x and y are the parameters.

3.2. **Diagram of possible orientations.** Remember that a candidate surface F is the result of gluing 2-manifolds $F_i \subset B_i$. So, it will be necessary to determine when F_i is orientable, and later, when the gluing of all F_i match together in order for F to be orientable too.

When the surface F_i is orientable, all its intersections with the levels $S_i \times \{t\}$ in the collar near ∂B_i can be described using a parametrized oriented train track T_i^t where the possible orientations of F_i are the parameters. In the construction process, we will only know the part of F_i inside the ball boundary by the level sphere $S_i \times \{t\}$; we will denote it by F_i^t. When this part is orientable, we can describe T_i^t as a parametrized train track.

In general F_i^t will be disconnected and we will have two possible orientations per connected component of F_i^t. For each possible orientation of F_i^t we will have an orientation for the train track diagram T_i^t. But, we can identify all the possible orientation of F_i^t with the elements of $\{1.-1\}^{|F_i^t|}$ ($|X|$ denotes the number of components of X). We will call *diagram of possible orientations* to the set of orientations of a diagram T_i^t parametrized by the possible orientations of F_i^t. Fig. 14 shows an example of a diagram of possible orientations. A simple way of seeing this diagram, is as a diagram of orientations but instead of ± 1 we use variables.

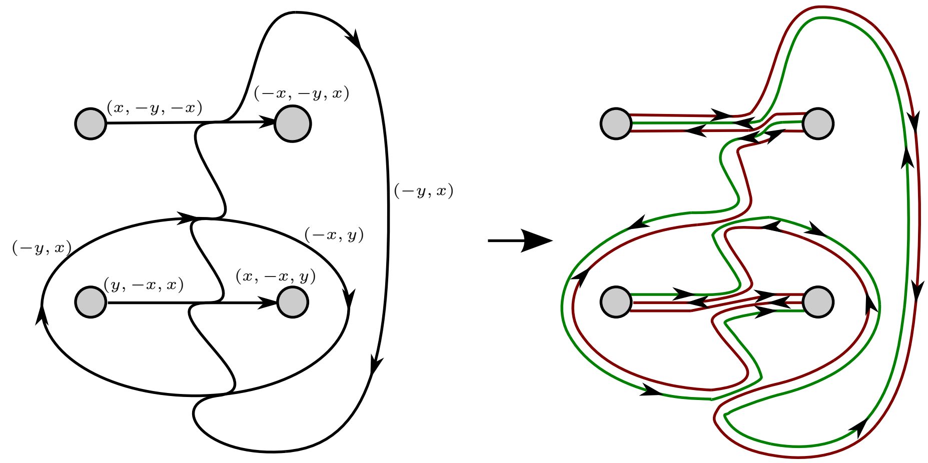

FIGURE 14. Example of a diagram of possible orientations

We will refer to the diagram of possible orientations of F_i as the diagram of possible orientations of F_i^t when $t = 1$.

So now, in order to get an orientable manifold when we glue all the 2-manifolds F_i, each pair of diagram of possible orientations of T_i and T_{i+1} must satisfy a set or relations between their parameters. Each relation is of the type $x_j = \pm y_l$, where x_j is a parameter that defines the orientation of some arc in T_i that glues with another arc in T_{i+1} whose orientation is defined by y_l.

3.3. **Orientations of each F_i.** In order to understand the effect of a saddle on the orientabillity of a surface we are going to consider the branched covering determined by the projection $\mathbb{R}^2 \to \mathbb{R}^2/G$ where G is the group generated by the 180 rotations with center on $\mathbb{Z}^2 \subset \mathbb{R}^2$. Notice that $\mathbb{R}^2/G$ is a sphere and $\mathbb{R}^2 \to \mathbb{R}^2/G$ has four points of ramification.

Now, think of $\mathbb{R}^2/G$ as a sphere with four holes (the ramifications points); then any pair of arcs of slope p/q lifts to lines of slope p/q with rational coordinates on $\mathbb{R}^2$.

On this projection, any two points (x_0, y_0) and (x_1, y_1) are projected to the same point if and only if $x_0 - y_0$ and $x_1 - y_1$ are even integers. And $\mathbb{Z}^2$ projects to the points of ramification (the four holes), so we are going to name the four holes of $\mathbb{R}^2/G$ as an element of its preimage; in particular we are going to name them as $(0,0), (1,0), (0,1)$ and $(1,1)$ (Fig. 15 shows the names on a train track).

Suppose that a saddle transforms a pair of arcs of slope p/q into another pair of arcs u/v. After lifting both pairs of arcs, we can observe that the the parallelogram $(-q,-p), (q,p), (v+q, u+p), (v-q, u-p)$ is a fundamental region for the branched

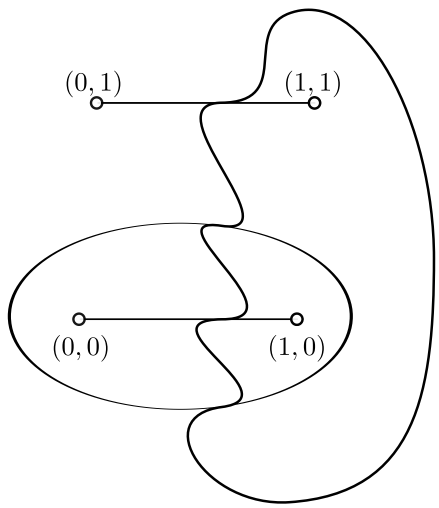

Figure 15. Vertex notation.

covering. The two possible saddles that transform p/q to u/v lift into the ones shown in Fig. 16; one is on the half parallelogram $(0,0),(q,p),(q+v,p+u),(v,u)$ (named s_1) and the other is on the other half parallelogram (named s_2).

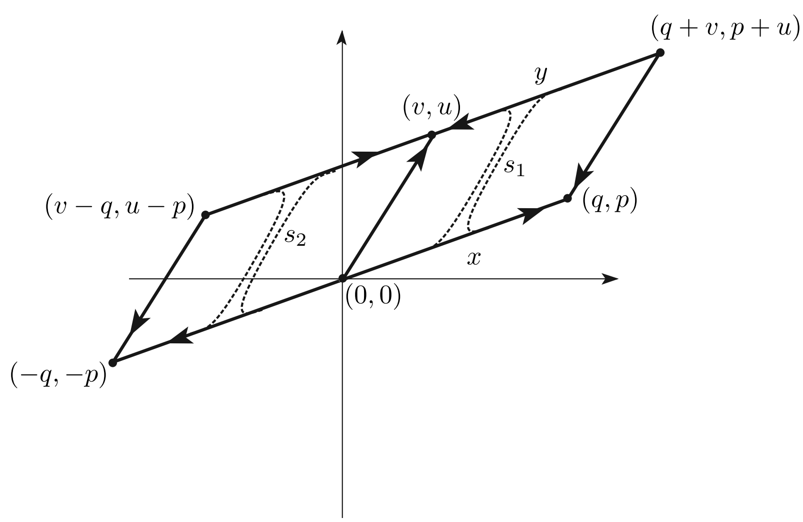

Figure 16. A fundamental region of the branch covering $\mathbb{R}^2 \to \mathbb{R}^2/G$ and the lift of saddles

On Fig. 16 we can observe that when we transform a pair of arcs into another, the transformed arcs pass through slope infinity on the vertices corresponding to obtuse angles. That is, on Fig. 16, when transforming using the saddle s_1 the slope infinity occurs on vertices (v,u) and (q,p); and when using s_2 slope infinity happens on vertices $(0,0)$ and $(v-q,u-p)$. And moreover, this change happens on clockwise direction around those vertices regardless of the saddle choice. This pass through slope infinity will be projected on $\mathbb{R}^2/G$ as a twist around the corresponding holes.

In addition, if we think of x and y as parallel copies of an arc, then s_1 will identify the first copy of x with the first of y; but if we use s_2, the last copies of x and y are the ones that are going to be identified.

Fig. 16 is depicting the case when $p/q < u/v$. So, when we change the figure for the other case ($p/q > u/v$) we can mostly make the same observations as before; only few things change, like the directions of the twist.

We can summarize this analysis on Table 3.3; this table has all the possibilities.

Saddle effects: twist and parallel arcs connectivity.

$\times$	$p/q < u/v$	$p/q > u/v$
twist direction	Clockwise	Counter-clockwise
s_1	Twist around (q, p) and (v, u)	
$\times$	Identify **leftmost** parallel arcs	Identify **rightmost** parallel arcs
s_2	Twist around $(0, 0)$ and $(v - q, u - p)$	
$\times$	Identify **rightmost** parallel arcs	Identify **leftmost** parallel arcs

One more thing to notice is that the table describes what is happening on the projection. We only need to make modulo two reduction on the vertices. We will prefer to use vertex $(v + q, u + p)_{\text{ mod } 2}$ instead of $(v - q, u - p)_{\text{ mod } 2}$, just for simplicity.

3.3.1. *Edgepaths of length less than or equal to 1.* Using the diagram of possible orientations we need to describe what happens after passing across a saddle; and more importantly, we need to determine if F_i is still orientable. We almost answer this question with the analysis made on the previous section. And we only need to write down those observations in terms of oriented train tracks.

Consider a train track corresponding to a point on a non horizontal edge or on the edge $\langle \infty, 0/1 \rangle$. Its orientations are determined by the orientations of the edges incident to the holes.

Now, we are going to focus on determining the possible orientations of these edges. This means we describe the possible assigned weights on any orientation of these edges. We will say that the edge is oriented pointing *out* if the hole is at the start of the edge; otherwise we say it is oriented pointing *in*.

In the following theorem, we are going to use the notation shown on Fig. 15 to denote the four vertices of a train track diagram. And also, we are going to need $\rho : \mathbb{P}_2 \to \mathbb{P}_2$ the permutation function given by

$$\rho(x_1, x_2, \ldots, x_n) = (x_2, x_3, \ldots, x_n, x_1)$$

for all n.

Remark 3.4. From now on, we will be using the function ρ and the function J (see Remark 3.1) on most of the equations, so it is important to keep their definition at hand.

Theorem 3.5. *Let F be the part of an m sheet candidate surface, inside a tangle and associated to an edgepath contained on $\langle p/q, u/v \rangle$ (a non-horizontal edge of $\mathcal{D}$) that starts in $\langle p/q \rangle$ and ends in the point*

$$\frac{m - \alpha}{m} \langle p/q \rangle + \frac{\alpha}{m} \langle u/v \rangle$$

, where α is any integer that satisfies $1 \leq \alpha \leq m$. Then:

(1) *F is orientable and unique up to isotopy.*
(2) *F has $2m - \alpha$ connected components.*
(3) *The diagram of possible orientations near the four holes, can be described by the next table*

Vertex	*Diagram Orientation*	*Weight*
$(0,0)$	*Out*	$\rho^{\pm\alpha}(x)$
$(q+v, p+u)_{\text{ mod } 2}$	*Out*	$\rho^{\pm\alpha}(y)$
$(q,p)_{\text{ mod } 2}$	*In*	x
$(v,u)_{\text{ mod } 2}$	*In*	y

where the sign of the exponent on ρ would be positive if $p/q > u/v$, and negative otherwise. The weights $x = (x_1, x_2, \ldots, x_n)$ and $y = (y_1, y_2, \ldots, y_m)$ satisfy $x_i = y_i$ ($i = 1, \ldots, \alpha$) if $p/q > u/v$ and $x_{m-i} = y_{m-i}$ ($i = 0, \ldots, \alpha - 1$) if $p/q < u/v$.

Proof. Remember that in the process of construction of F we have two options for every saddle, these two types of saddles are level interchangeable. And also, we can push the initial saddle across the ball bounded by $\partial B \times 0$ and change its type. This implies, that all the possibilities of F are isotopic.

Now, we can think F is obtained from the edgepath with all its α saddles parallel between them (i.e. all of the same type). Each saddle joins one pair of arcs of slope p/q and transforms it into a pair of slope r/s, reducing the number of components of F by one. And also, there are no orientability problems, because each arc belongs to a different component. So, F is orientable and has $2m-\alpha$ connected components.

If we project the arcs x and y shown on Fig. 16, the orientation will be near each point like in Fig. 17 a. For simplicity, we are going to write $(a,b)_2$ to denote the pair with modulo two reduction.

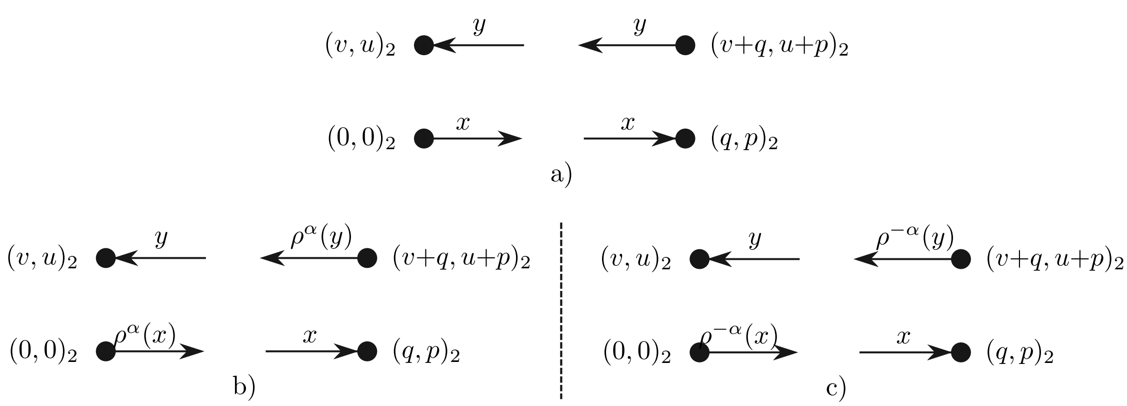

FIGURE 17. Orientation near vertices

Suppose that $p/q > u/v$; by Table 3.3, after saddle s_2, the leftmost arc of x is joined with the leftmost arc of y and a twist will occur around vertices $(0,0)$ and $(v-q, u-p)_2 = (v+q, u+p)_2$. This means that $x_1 = y_1$ and that the weights near $(0,0)_2$ and $(v+q, u+p)_2$ will be changed to $\rho(x)$ and $\rho(y)$, respectively. More generally, after passing across α saddles of type s_2, we will end up with $x_i = y_i$ for

$i = 1, \ldots, \alpha$ and the weights near $(0,0)$ and $(v+q, u+p)_2$ will be changed to $\rho^\alpha(x)$ and $\rho^\alpha(y)$, respectively (see Fig. 17 b).

In the case that $p/q < u/v$, after passing across α saddles of type s_2 we will end up with $x_{m-i} = y_{m-i}$ for $i = 0, \ldots, \alpha - 1$ and the weights as in Fig. 17 c.

From the last two paragraphs part (3) follows. □

3.3.2. *Monochromatic edgepaths.* We can color all the edges of diagram $\mathcal{D}$ with three colors; one for each type of modulo two reduction of its end points: $\langle 1/0, 1/1\rangle$, $\langle 1/1, 0/1\rangle$ and $\langle 0/1, 1/0\rangle$.

We will say that an edgepath is monochromatic if all edges are of the same color.

Theorem 3.6. *Let F be a 2 -manifold obtained from a monochromatic edgepath Γ, with length grater or equal than one. Suppose its last segment starts at $\langle u/v\rangle$ and ends at a point of projective coordinates:*

$$\frac{m-\alpha}{m}\langle\frac{u}{v}\rangle + \frac{\alpha}{m}\langle\frac{u'}{v'}\rangle$$

for some $0 < \alpha \leq m$. Then, the diagram of orientations for F is described by the following table:

Vertex	*Diagram Orientation*	*Weight*
$(0,0)$	*Out*	y
$(v,u)_2$	*In*	$\rho^{\pm\alpha}(y)$
$(v',u')_2$	*In*	$\rho^{\pm\alpha}(y)$
$(v+v', u+u')_2$	*Out*	y

The sign of the exponent over ρ is positive if $u/v < u'/v'$ and negative otherwise.

Proof. We are going to proceed by induction on the length of $|\gamma| \geq 1$ which is possible by considering m as a constant and observing that $m|\gamma|$ has to be a positive integer. Or equivalently, we are proceeding by induction on the number of saddles defined by γ, but we have at least m saddles.

When $|\gamma| = 1$ the result is a direct consequence of theorem 3.5 in the case $\alpha = m$.

Assume that the result is true for certain value of $|\gamma| = \beta \geq 1$. Now we are going to prove that the result is true for $|\gamma| = \beta + 1/m$. That is, we are going to prove that the result is still true after adding a saddle.

We have two cases depending on whether β is an integer or not.

Case β is an integer. Let γ' be the edge path resulting from γ after removing the last $1/m$ fraction of edge; this implies that $|\gamma'| = \beta$.

By the induction hypothesis γ' satisfies the result, and as we are assuming that $|\gamma'|$ is an integer its end point has to be a vertex, and that means we have to use $\alpha = m$ for the theorem conditions. So, the following table describes the diagram of orientations for γ'

Vertex	Diagram Orientation	Weight
$(0,0)$	Out	y
$(v,u)_2$	In	y
$(v',u')_2$	In	y
$(v+v', u+u')_2$	Out	y

Notice that $\rho^{\pm 1}(y) = y$ because y has length m.

Now, to complete γ we need to add a fraction of an edge to γ'; that fraction starts at $\langle u'/v'\rangle$ and ends at a point of the form

$$\frac{m-1}{m}\langle\frac{u'}{v'}\rangle + \frac{1}{m}\langle\frac{u''}{v''}\rangle$$

this means adding a saddle.

Because γ is monochromatic we get that $(v'', u'')_2 = (v, u)_2$. This implies that the diagram at Fig. 16 would keep the same orientation. So, Table 3.3 would apply in this case, and the twist would occur on the same pair of vertices as before, and the leftmost relations would translate to $x_1 = x_1$ and rightmost to $x_n = x_n$ adding superfluous relations.

If we pass through a saddle of type s_1 (see Table 3.3), it creates a twist on $(v', u')_2 = (q, p)_2$ and changing their corresponding weights from y to $\rho(y)$ if $u'/v' < u''/v''$ and to $\rho^{-1}(y)$ otherwise. Thus, the theorem is true in this case.

But if we go through the saddle (of type s_2) the weight at the edges near $(0, 0)_2$ and $(v' + v'', u' + u'')_2$ would change to $\rho^{\mp1}(y)$; the exponent is negative if $u'/v' < u''/v''$ and positive otherwise. Now, changing the variable y by $\rho^{\pm1}(x)$ means to replace on the train track diagram $\rho^{\mp1}(y)$ by x and y by $\rho^{\pm1}(x)$; thus, we would get the conclusion of the theorem.

Case β is not an integer. In this case the end point for γ' (the edgepath $1/m$ of smaller length then γ) has the form

$$\frac{m-\alpha}{m}\langle\frac{u}{v}\rangle + \frac{\alpha}{m}\langle\frac{u'}{v'}\rangle$$

for some $0 < \alpha < m$. So, the end point of γ would be the same but with $\alpha + 1$ instead of α. This is again a one saddle increase.

By induction hypothesis, the diagram of orientations associated to the γ' edgepath is the one on the statement of this theorem. Now we are going to study how these weights changed after adding a saddle.

The effect of the saddle can be understood by analyzing the branch covering in Fig. 16 but with $x = y$. By Table 3.3, it is clear that if the saddle is s_1 the weights on $(v, u)_2$ and $(v', u')_2$ are going to change to $\rho^{\pm(\alpha+1)}(y)$. Thus, the theorem is satisfied in this case.

The remaining case is when the saddle is s_2. Here, the saddle affects the weights on $(0, 0)$ and $(v + v', u + u')_2$, changing them from y to $\rho^{\mp1}(y)$ (the sign depending on whether $u/v < u'/v'$ or not). But, by changing the variable $\rho^{\mp1}(y)$ by x (in consequence, changing $\rho^{\pm\alpha}(y)$ to $\rho^{\pm(\alpha+1)}(x)$) we get that the Theorem is also satisfied in this case, finishing the last step of the induction.

□

3.3.3. *Non-Monochromatic edgepaths.* As we saw in the previous subsection, the number of components of a 2-manifold described by a monochromatic edgepath is greater then or equal to m. We are going to see that the number of components will be reduced in the case that the edgepath is not monochromatic.

Let us start considering the case when the edgepath is *quasi-monochromatic*, that is, when the edgepath is monochromatic when removing the last edge and this last edge is of a different color.

Theorem 3.7. *Let γ be a quasi-monochromatic edgepath. Let $\langle u_0/v_0, u_1/v_1\rangle$ and $\langle u_1/v_1, u_2/v_2\rangle$ be the last two edges through which it passes.*

Then, the diagram of orientations of the associated surface could be described by the following table.

Vertex	*Diagram Orientation*	*Weight*
$(0,0)$	*out*	$\rho^{\varepsilon r}(x)$
$(v_0,u_0)_2$	*in*	$\rho^{-\varepsilon r}(x)$
$(v_1,u_1)_2$	*in*	$\rho^{-\varepsilon s}(x)$
$(v_2,u_2)_2$	*out*	$\rho^{\varepsilon s}(x)$

where r is the number of saddles of the type that twist around $(0,0)$ and s is the amount of saddle of the other type, and ε is the sign of $u_1/v_1 - u_2/v_2$. Moreover, $x_i = -x_{m+1-i}$ for $i = 1, \ldots, max\{r,s\}$.

Proof. Consider γ', the monochromatic edgepath resulting from removing the last edge of γ. From Theorem 3.6 we can get the diagram of orientations for γ', which is described by the following table:

Vertex	Diagram Orientation	Weight
$(0,0)$	out	x
$(v_0,u_0)_2$	in	x
$(v_1,u_1)_2$	in	x
$(v_2,u_2)_2$	out	x

Consider now the branched covering studied in Section 3.3 and the fundamental region delimited by the slopes u_1/v_1 and u_2/v_2. Now, lift the diagram of orientations of γ' to this covering, which will look as in Fig. 18.

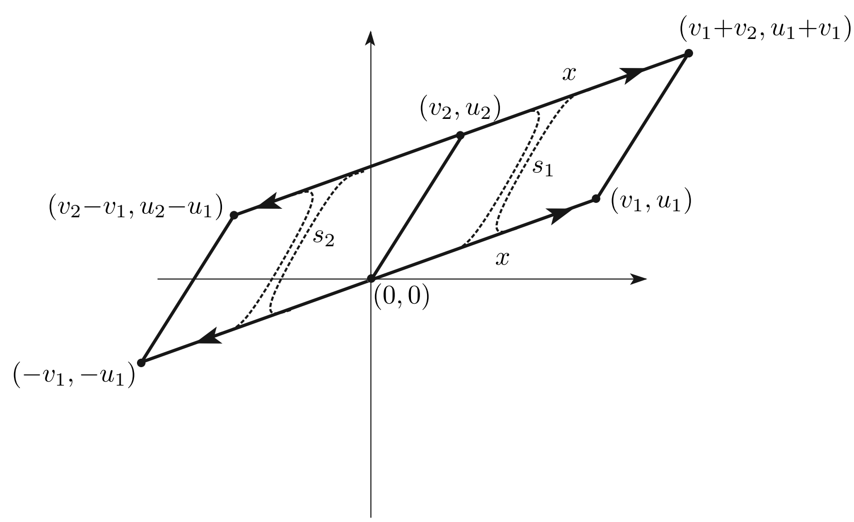

FIGURE 18. Lift of arcs with $u_1/v_1 < u_2/v_2$

So, similarly to Table 3.3 we can describe the effects of saddles s_1 and s_2; and we would need to separate the cases $u_1/v_1 < u_2/v_2$ and $u_1/v_1 > u_2/v_2$.

The table on this theorem summarizes all these possibilities.

As we can observe in Fig. 18, regardless which saddle is chosen, the leftmost arc of slope u_1/v_1 is identified with the corresponding rightmost arc of the same slope; meaning that the last entry of x is equal to the first one. So, if we apply the same saddle (let say s_2) r times it will imply that $x_i = x_{m+1-i}$ for $i = 1, \dots, r$. But, if we pass through both saddles, the same relation on x will be implied; that is $x_1 = x_{m+1-i}$ with one saddle and $x_{m+1-i} = x_i$ with the other. So, if we pass through s saddles of one type and r saddles of the other, we get the relations $x_i = -x_{m+1-i}$ for $i = 1, \dots, \max\{r, s\}$. □

An important corollary of Theorem 3.7 is the following.

Corollary 3.8. *No edgepath associated to an ICON surface can contain two full edges of different color.*

Proof. Consider γ, an edgepath with two edges of different color. Take the first edge where γ changes of color; and only consider the part of γ until that edge.

So, applying the previous theorem (3.7) and the fact that the full last edge belongs to γ, then we will have $r + s = m$. As γ is associated to an ICON surface, m must be odd. So, either r or s must be greater than or equal to half of m. That is, $\max\{r, s\} \geq (m + 1)/2$.

Hence the identity $x_i = -x_{m+1-i}$ must hold for $i = (m + 1)/2$, ie, $x_{(m+1)/2} = -x_{(m+1)/2}$. Therefore, $x_{(m+1)/2}$ should be zero, preventing the existence of solutions in $\{1, -1\}$. □

The previous corollary means that, for ICON surfaces there are only monochromatic or quasi-monochromatic edgepaths.

3.4. **Final gluing for type II surfaces with monochromatic edgepaths.** In this section we study the final step in the construction of candidate surfaces for a specific case, helping us to discard several possibilities in the following chapters.

Theorem 3.9. *A candidate surface of type II generated from monochromatic edgepaths $\gamma_1, \gamma_2, \dots, \gamma_n$ of color $\langle 1/1, 0/1\rangle$ is connected if and only if the leaf number m is exactly one.*

Proof. Suppose that the edgepath γ_i ends at the point:

$$\frac{m - a_i}{m}\langle k_i\rangle + \frac{a_i}{m}\langle k_i + 1\rangle$$

with k_i an integer and a_i a non-negative integer smaller than m.

Because γ_i is monochromatic, we can apply Theorem 3.6 and obtain the diagram of orientations shown on Fig. 19. This diagram is independent of whether γ_i goes down from $\langle k\rangle$ to $\langle k + 1\rangle$ or goes up from $\langle k + 1\rangle$ to $\langle k\rangle$.

In order to keep orientability, the following relationships must be satisfied at the vertices:

$$\rho^{a_i}(x_i) = x_{i+1} \qquad i = 1, 2, \dots, n \tag{2}$$

Finding a solution to the previous system of equations is equivalent to finding a solution x_1 to the equation $\rho^{a_1+a_2+\cdots+a_n}(x_1) = x_1$. But, because the ordinates of the endpoints add up to zero, it means that $a_1 + a_2 + \cdots + a_n$ is a multiple of m, and so $\rho^{a_1+a_2+\cdots+a_n} =$ identity. Hence, for every value of x_1 we can create a solution for the system 2.

Let $\{x_1, x_2, \dots, x_n\}$ be a solution of the system (2). Then, when gluing the two half-planes as in Fig. 20 the orientations of all their arcs will match perfectly. This

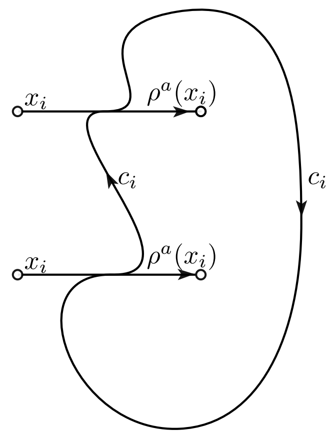

FIGURE 19. Diagram of orientations for F_i

is explained by the fact that the train track of a half-plane, like the one in Fig. 20 a), depends entirely on the value of the weights near its vertices.

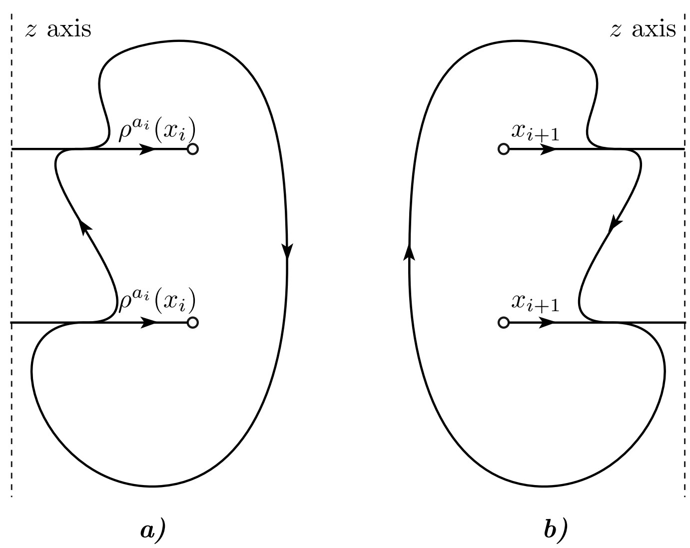

FIGURE 20. Half diagram with $b = 0$

The last argument proves that for every value of x_1 we create an orientation for the candidate surface, but because an ICON surface is orientable and connected, there should be only two possible orientations. So, the length of the weight $x_1 \in \{1, -1\}^m$ has to be equal to one; i.e $m = 1$. □

4. ICON SURFACE IN THE EXTERIOR OF THE PRETZEL KNOTS $P(p.q.-r)$

It is easy to see that CON surfaces are necessarily connected, have zero boundary slope and an odd number of boundary components. In this chapter we will apply

Slopes for all the possible edgepaths.

$-\frac{1}{r}$ $\frac{1}{q}$ $\frac{1}{p}$	II	III
$+++$	$4-2(p+q)$	$-2(p+q)$
$++-$	$2-2p$	$-2p$
$+-+$	$2-2q$	$-2q$
$+--$	0 *	0 *
$-++$	$2-2(p+q-r)$ *	$-2(p+q-r)$
$-+-$	$2(r-q)$ *	$2(r-q)$ *
$--+$	$2(r-p)$ *	$2(r-p)$ *
$---$	$2r-2$	$2r$

the Hatcher and Oertel algorithm from [**?**] to the pretzel knots $P(p,q,-r)$ with p, q and r odd numbers grater than 1; and we are going to determine the zero ∂-slope surfaces and determine which of those surfaces are connected with an odd number of boundary components.

There are only two minimal edgepaths from a vertex $\langle \pm 1/p\rangle$ to the left border of $\mathscr{S}$; one moving always upwards and the other downwards. So, for the three tangles there would be $2^3 = 8$ combinations. We write these as, e.g., $++-$, meaning: the upward edgepaths in the first two tangles and the downward edgepath in the third. We write these combinations in Table 4 as Hatcher and Oertel did at [**?**]. Recall that, for the computation of this table, the equation (1) is required and notice that $\tau(F_0) = 2$.

Notice that the cases which are not marked with * have non-zero ∂-slope.

4.1. **Candidate surfaces of type II.** Let us start by analyzing the candidate surfaces of type II. As we saw earlier there are only four possibilities in which the candidate surface may have zero ∂-slope.

- $+--$ The three edgepaths meet the y axis precisely at the vertex $0/1$.
- $-++$ can only give zero when $p+q-r=1$.
- $-+-$ Necessarily that $r=q$ to have zero ∂-slope. $[--+]$ is analogous to the previous case, so it requires that $r=p$.

Let us start with the simplest case; this is the second one $(-++)$. Since the sum of the ordinates of the edgepaths when they reach the y axis is 1, the edgepaths must be extended at least one edge downwards. But that downward extension cannot be performed on the paths $\gamma_{1/p}$ and $\gamma_{1/q}$, because it would pass through two consecutive edges of the same triangle. Then, extension must be made in the edgepath $\gamma_{-1/r}$. But this will imply that $\gamma_{-1/r}$ would have two full edges of different color, contradicting Corollary 3.8. Therefore, the surface in this case cannot be ICON.

In order of difficulty, the following case is the $+--$. On it, all the edges can be extended vertically in either direction (up or down) without contradicting the condition of minimality E2 (Definition 2.4) neither the condition of monochromaticity (Corollary 3.8). So, we will have many orientable candidate surfaces of slope zero. But, as the three edgepaths are monochromatic and of the color $\langle 1/1, 0/1\rangle$, they satisfy the conditions of Theorem 3.9. So, none of these candidate surfaces will be ICON with disconnected boundary.

It only remains the case $-+-$ (which is analogous to $--+$). The edgepaths γ_{-r} and γ_q are monochromatic of color $\langle 1/0, 1/1\rangle$ and if they are extended vertically, this will imply that γ_{-r} and γ_q are quasi-monochromatic; in both edgepaths we can use Theorem 3.7 and obtain their diagrams of orientations; both will look like Fig. 21 a). As the path γ_p is monochromatic, we can use the table in Theorem 3.6 to describe its diagram of orientations (Fig. 21 b).

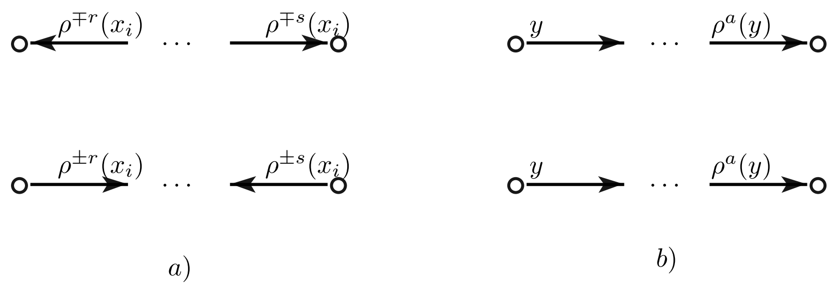

FIGURE 21. Diagram of orientations near the holes for the case $+-+$.

Now, in order to keep orientability, when we glue the two diagrams from Fig. 21, the relations $\rho^{\mp s}(x) = y$ and $\rho^{\pm s}(x) = -J(y)$ must be satisfied. But, combining these two last identities we get that

$$\begin{aligned}\rho^{\pm s}(x) &= -J(\rho^{\mp s}(x))\\ \rho^{\pm s}(x) &= -\rho^{\pm s}(J(x))\\ x &= -J(x) \qquad (3)\end{aligned}$$

But as $|x| = m$ must be odd (to be ICON) and by 3 the middle entry of x should be zero. Therefore, the system has no solution in $\{1, -1\}^m$ and therefore the obtained candidate surface shall be non-orientable.

In summary, throughout this section we have proved the following statement.

Proposition 4.1. *In the pretzel knots $P(p, q, -r)$ with p, q and r odd integers greater than 1, there are no ICON candidate surfaces of type II, with disconnected boundary.*

4.2. **Candidate surface of type III.** Type III candidates surfaces for cases $-+-$ and $--+$ are compressible by Proposition 2.5 (b) in [**?**]. This is because the path $\gamma_{-1/r}$ will be completely reversible and $\sum_i k_i = 0$ (see [**?**]).

For the case $+--$ we will have to do a bit more work. In this case, all paths shall terminate at the same point in the edge $\langle 0/1, \infty\rangle$. So, we can say that all three edges end at the following point:

$$\frac{m-k}{m}\langle 0/1\rangle + \frac{k}{m}\langle\infty\rangle$$

where k is an integer between $0 < k < m$.

First observe that the saddles that transform slope $\langle 0/1\rangle$ into $\langle\infty\rangle$ are the ones shown in Fig. 22 a). And if we use r_i of one type and s_i of the other, the diagram of orientation will be the one shown on Fig. 22 b), and the first $\max\{r_i, s_i\}$ coordinates of x_i are equal to the negative of the last ones; more precisely, we can write $x_i = z_i \oplus y_i \oplus -J(z_i)$ where $|z_i| = \max\{r_i, s_i\}$

It is not hard to see, that if $s_1 = s_2 = s_3$ (consequently $r_1 = r_2 = r_3$) then, the candidate surface will be disconnected. So, without loss of generality we can say that $m/2 > s_1 > s_2 > 0$

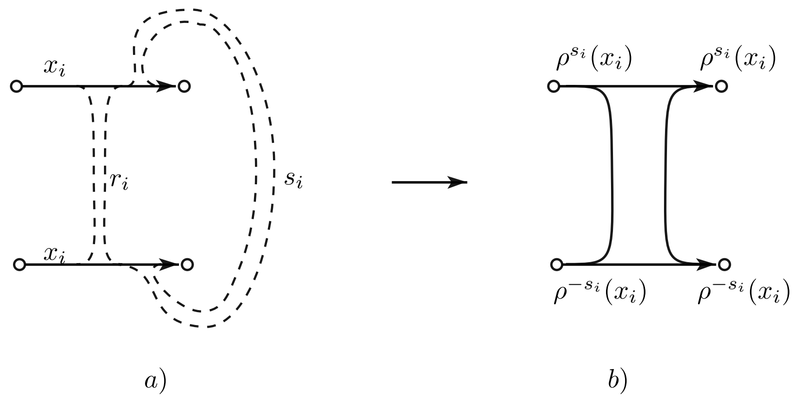

FIGURE 22. Train track with final point $\frac{m-k}{m}\langle 0/1\rangle + \frac{k}{m}\langle\infty\rangle$

Now, gluing these last two train tracks, we get the relations $\rho^{s_1}(x_1) = \rho^{s_2}(x_2)$ and $\rho^{-s_1}(x_1) = \rho^{-s_2}(x_2)$; combining these two we get that $\rho^{2(s_1-s_2)}(x_1) = x_1$. By definition $\rho^m(x_1) = x_1$ in consequence we have that:

$$\rho^g(x_1) = x_1 \qquad \text{where } g = \text{g.c.d}(m, s_1 - s_2) \tag{4}$$

Let w_1 be the subarray of z_1 formed by its first g coordinates; that is, $z_1 = w_1 \oplus h_1$. Then $w_1 \oplus h_1 \oplus y_1 \oplus J(-h_1) \oplus J(-w_1) = x_1 = \rho^g(x_1) = h_1 \oplus y_1 \oplus J(-h_1) \oplus J(-w_1) \oplus w_1$; this implies that $J(-w_1) = w_1$. But $|w_1| = g$ is odd; so the middle coordinate of w_1 should be zero, implying that there is no solution in $\{1, -1\}$.

We have proven the following proposition.

Proposition 4.2. *In the pretzel knots $P(p, q, -r)$ with p, q and r odd integers greater than 1, there are no ICON candidate surfaces of type III with disconnected boundary.*

4.3. **Candidate surfaces of type I.** Let us start by remembering that there are several possibilities for the paths γ_p, γ_q and γ_{-r}. Such possibilities can only move from right to left in the highlighted part of Fig. 23. Fig. 23 a) shows the possibilities for path γ_p (a similar figure applies to the edgepath γ_q) and Fig. 23 b) shows the possibilities for γ_{-r}.

As we are in the case of type I candidate surfaces, we need to find $x \in (0, 1)$ such that $\gamma_p(x) + \gamma_q(x) + \gamma_{-r}(x) = 0$ where γ_i can be the function γ_i^+, γ_i^- or the constant path for $i = p, q, -r$. Each of these functions can be given precisely:

$$\gamma_i^+(x) = 1 - x \qquad \text{for } i = p, q \text{ and } x \in [0, i - 1/i) \tag{5}$$
$$\gamma_i^-(x) = x/(i-1) \qquad \text{for } i = p, q \text{ and } x \in [0, i - 1/i) \tag{6}$$
$$\gamma_{-r}^+(x) = -x/(r-1) \qquad \text{for } x \in [0, r - 1/r) \tag{7}$$
$$\gamma_{-r}^-(x) = x - 1 \qquad \text{for } x \in [0, r - 1/r) \tag{8}$$

We are going to proceed by cases. Let us begin with the case where all the edgepaths are constant.

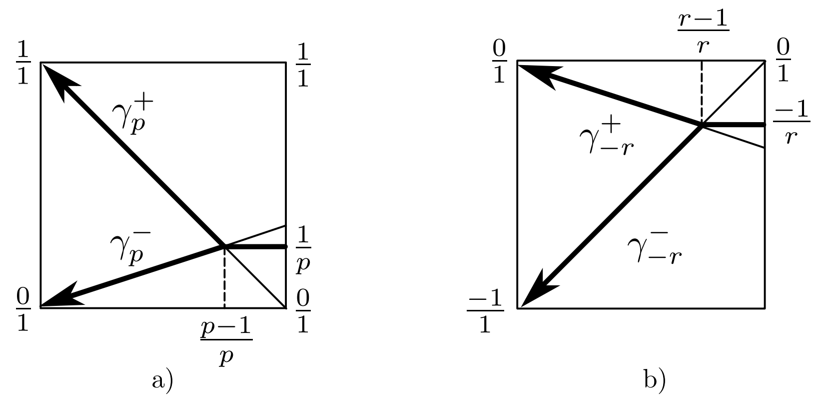

Figure 23. Type I edgepaths

Solutions of $\gamma_p(x) + \gamma_q(x) + \gamma_{-r}(x) = 0$.

$\frac{1}{p}$	$\frac{1}{q}$	$-\frac{1}{r}$	Solution on x
$+$	$+$	$+$	$(2r-2)/(2r-1)$*
$+$	$+$	$-$	1
$+$	$-$	$+$	$(rq-r-q+1)/(rq-2r+1)$*
$+$	$-$	$-$	0
$-$	$+$	$+$	$(rp-r-p)+1)/(rp-2r+1)$*
$-$	$+$	$-$	0

Proposition 4.3. *For the pretzels $P(p,q,-r)$ with p, q and r odd integers grater than 1, there are no type I candidate surfaces with three constant paths.*

Proof. On this case the equation $\gamma_p(x) + \gamma_q(x) + \gamma_{-r}(x) = 0$ will be equivalent to $1/p + 1/q = 1/r$, but this is impossible because p, q and r are odd. □

Now we study what happens if none of the edgepaths is constant. In the following lemma we will discard most of the cases. The right inequality in condition (9) follows from the fact that edgepaths are not constant (see the possible values of x on equations 5, 6, 7 and 8) and the left inequality follows from the type I condition on the candidate surface.

Lemma 4.4. *If none of the paths γ_* is constant, then the equation $\gamma_p(x)+\gamma_q(x)+\gamma_{-r}(x) = 0$ will have a solution in x with*

$$0 < x < min\left\{\frac{q-1}{q}, \frac{p-1}{p}, \frac{r-1}{r}\right\} \tag{9}$$

only if $\gamma_p(x) = \gamma_p^-(x) = x/(p-1)$ and $\gamma_q(x) = \gamma_q^-(x) = x/(r-1)$.

Proof. As each edgepath γ_* has two possibilities, 8 cases need to be considered. In order to prove the proposition, we only need to discard them all but cases $--+$ and $---$; that is, when $\gamma_p = \gamma_p^-$, $\gamma_q = \gamma_q^-$ and γ_r any of the two possibilities.

For each case (excluding the two exceptions), $\gamma_p(x) + \gamma_q(x) + \gamma_{-r}(x) = 0$ will be a linear equation with unique solution (not necessarily satisfying condition (9)). On the following table we write the solutions for every case:

By the condition (9), x cannot be 1 or 0. So, there only remain the possibilities marked with asterisk. But condition (9) fails for those too, as we will show below:

- For the case $+++$ we can notice that: $(2r-2)/(2r-1) < \frac{r-1}{r} \Leftrightarrow 2r < 2r-1$; which is impossible.
- For the case $+-+$ we use that $(rq-r-q+1)/(rq-2r+1) < \frac{r-1}{r} \Leftrightarrow r < 1$; but this is impossible because r is a positive odd integer.
- Case $-++$ is analogous to the previous one.

□

Now using Lemma 4.4 we can prove the following proposition.

Proposition 4.5. *Candidate surfaces of type I for the Pretzel $P(p, q, -r)$ and associated to non-constant edgepaths are not ICON.*

Proof. By Lemma 4.4 there are only two cases that remain:

- Case $--+$ means that $\gamma_r = \gamma_r^+$. So the equation $\gamma_p(x)+\gamma_q(x)+\gamma_{-r}(x) = 0$ will have a non trivial solution if and only if

$$\frac{1}{p-1} + \frac{1}{q-1} = \frac{1}{r-1}$$

In that case, all rational x where $0 < x < 1 - \max\{1/p, 1/q, 1/r\}$ are solutions. Let x_0 be a rational value of x. The number of sheets (m) must satisfy that $\alpha_p = mx_0/(p-1)(1-x_0)$, $\alpha_q = mx_0/(q-1)(1-x_0)$ and $\alpha_r = mx_0/(r-1)(1-x_0)$ are integers. So, we can write the end point of each edgepath γ_i as follows:

$$\frac{\alpha_i}{m}\langle\frac{1}{i}\rangle + \frac{\beta_i}{m}\langle 0\rangle \tag{10}$$

where i is one of p, q or r and $\beta_i = m - \alpha_i$. We can notice, that by definition $\alpha_p + \alpha_q = \alpha_r$.

Applying Theorem 3.5 we can see that the diagrams of orientations of γ_p. γ_q and γ_r look like the ones of Fig. 24, where $|a_i| = \beta_i$, $|z_i| = |w_i| = \alpha_i$.

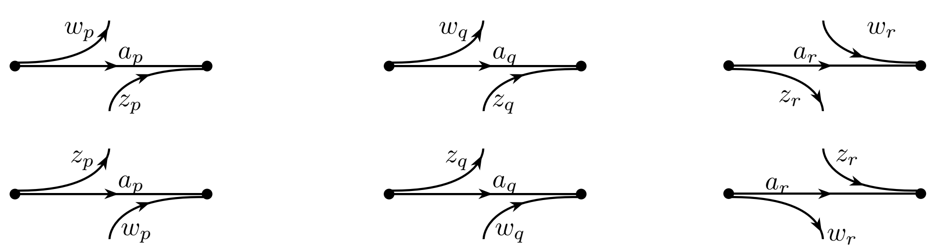

FIGURE 24. Diagrams of orientations for a Type I candidate surface when $\gamma_p = \gamma_p^-$, $\gamma_q = \gamma_q^-$ and $\gamma_r = \gamma_r^+$

By observing these diagrams, we can see that the first arc of a_q glues with the first arc of a_r on the tangle $1/r$, and also glues to the $(\alpha_q + 1)$-th arc of a_p. And, the first arc of a_r glues to the $(\alpha_r - \alpha_p + 1)$-th arc of a_p. But $\alpha_r - \alpha_p + 1 = \alpha_q + 1$, so the gluing actually closes a surface; this means that the candidate surface is disconnected.

Possibilities for γ_q and γ_{-r} when they are not constant and γ_p is constant a

Case	$\gamma_q(x)$	$\gamma_{-r}(x)$	Affirmation
$++$	$1-x$	$\frac{-x}{r-1}$	There is no solution with $x<1$
$+-$	$1-x$	$x-1$	There is no solution on x
$-+$	$\frac{x}{q-1}$	$\frac{-x}{r-1}$	The solutions correspond to nonzero slope
$--$	$\frac{x}{q-1}$	$x-1$	There is no solution with $x<(q-1)/q$

- Case $---$. In this case $\gamma_r(x) = x-1$. Let x_0 be the solution of the equation $\gamma_p(x)+\gamma_q(x)+\gamma_{-r}(x) = 0$, that is, $x_0 = (p-1)(q-1)/(pq-1)$. This solution will be in the required interval if and only if $r > 1/(1-x_0)$.

  Now, the edgepath γ_p ends at the point with coordinates $(x_0, x_0/(p-1))$, that is the point
  $$\frac{q-1}{p+q-2}\langle 1/p\rangle + \frac{p-1}{p+q-2}\langle 0\rangle.$$
  So, $\tau(\gamma_p) = (p-1)/(p+q-2)$. Similarly, we can compute $\tau(\gamma_q) = (q-1)/(p+q-2)$.

  By substitution into the slope formula for candidate surfaces we got
  $$\text{slope} = 2-2(\tau(\gamma_p)+\tau(\gamma_q)+\tau(\gamma_{-r})) = -2\tau(\gamma_{-r})$$
  But, as the edge path γ_{-r} is not constant and always decreases, we must have $\tau(\gamma_{-r}) \neq 0$. So, the candidate surface has nonzero slope.

□

Now we will concentrate on the cases where two edgepaths are constants and the other not. Remember that the slope of a candidate surface is computed by $2-2(\tau(\gamma_p)+\tau(\gamma_q)+\tau(\gamma_{-r}))$. As we want this number to be zero and the two edgepaths to be constant, the nonconstant edgepath γ_i should have twist number equal to 1, that is, $\tau(\gamma_i) = 1$. Therefore γ_i has negative slope and travels a full edge which implies that $i = -r$, that is, γ_{-r} is the nonconstant edgepath.

Now, $\tau(\gamma_{-r}) = 1$ means that γ_{-r} goes from $\langle -1/r\rangle$ to $\langle -1/(r-1)\rangle$. The x-coordinate of the point $\langle -1/(r-1)\rangle$ is $x_0 = (r-2)/(r-1)$ and $\gamma_{-r}(x_0) = -1/(r-1)$. But x_0 has to be the solution of the equation $\gamma_p(x)+\gamma_q(x)+\gamma_{-r}(x) = 0$, which is equivalent to
$$\frac{1}{p}+\frac{1}{q} = \frac{1}{r-1}$$
but this is impossible due to the parity condition on p, q and r. We have therefore proved the following proposition.

Proposition 4.6. *There are no zero slope candidate surfaces for the pretzels $P(p,q,-r)$ with two constant edgepaths. Here, p, q and r are odd positive integers greater than 1.*

One last possibility is when one edgepath is constant and the other two are not.

Suppose that γ_p is the constant one, then we will have four possibilities for γ_q and γ_{-r}. For none of these possibilities there are candidate surfaces with zero slope.

Now, we are ready to prove the following proposition.

Proposition 4.7. *If the pretzel $P(p,q,-r)$ has an ICON surface with disconnected boundary then the surface must be described by a candidate surface of type I with the*

Possibilities for γ_p and γ_q when they are not constant and γ_{-r} is constant

Case	$\gamma_p(x)$	$\gamma_q(x)$	Assertion
++	$1-x$	$1-x$	$\tau(\gamma_*) < 0$ for $* \in \{p,q\}$, so the candidate surface has nonzero slope
+−	$1-x$	$\frac{x}{q-1}$	$\tau(\gamma_p) < 0$ and $\tau(\gamma_q) < 1$, so the candidate surface has nonzero slope
−+	$\frac{x}{p-1}$	$1-x$	analogous to previous case
−−	$\frac{x}{p-1}$	$\frac{x}{q-1}$	This is the only possibility

edgepath γ_{-r} constant with image $\langle -1/r\rangle$ and the other two are downward edgepaths. Moreover, the following relation must be satisfied:

$$\frac{1}{p-1}+\frac{1}{q-1}=\frac{1}{r-1}$$

Proof. By Propositions 4.1 and 4.2 the candidate surface must be of type I and by Propositions 4.5 and 4.6 the edgepath must have one and only one constant edgepath.

As we observed before, if γ_p or γ_q is constant there would be no candidate surface with zero slope. The remaining case is when γ_{-r} is constant and the other two edgepaths are not.

There are four possibilities for γ_p and γ_q, each one described on Table 4.3. The table discards all cases but $\gamma_p = \gamma_p^-$ and $\gamma_q = \gamma_q^-$.

Once we have defined the three edgepaths, we can compute the solution of $\gamma_p(x)+\gamma_q(x)+\gamma_{-r}(x) = 0$ and for that solution we can compute $\tau(\gamma_*)$. We need that $\tau(\gamma_p)+\tau(\gamma_q) = 1$ in order to have zero slope for the candidate surface. But this identity will be true if and only if

$$\frac{1}{p-1}+\frac{1}{q-1}=\frac{1}{r-1}$$

In this case, the solution of $\gamma_p(x)+\gamma_q(x)+\gamma_{-r}(x) = 0$ is $x_0 = (r-1)/r$; therefore the image of the edgepath γ_{-r} is exactly the point $\langle -1/r\rangle$. □

One last lemma to continue.

Lemma 4.8. *Let a, b and c be three positive integers such that*

$$\frac{1}{a}+\frac{1}{b}=\frac{1}{c}$$

. Then there are integers u, v and g such that $(u,v) = 1$ and

$$\begin{aligned} a &= gu(u+v)\\ b &= gv(u+v)\\ c &= guv \end{aligned} \tag{11}$$

Proof. Let $g = \gcd(a,b,c)$; then we can write $a = ga'$, $b = gb'$ and $c = gc'$ with a', b' and c' three integers without a common factor such that $1/c' = 1/a' + 1/b'$. Then let $h = \gcd(a',b')$, so we have $a' = hu$ and $b' = hv$ with u and v relatively prime integers. Making the appropriate substitutions we have

$$(u+v)c' = huv \tag{12}$$

As a', b' and c' have no common factors, $\gcd(h, c') = 1$, so c' must divide uv. Now, as $\gcd(u, v) = 1$ we will have $\gcd(u + v, uv) = 1$. In consequence $u + v$ must divide h. Hence

$$\frac{h}{u+v} \cdot \frac{uv}{c'} = 1. \tag{13}$$

Therefore, both factors have to be equal to 1; this means, $h = u+v$ and $c' = uv$. This concludes the proof. □

Now we are ready for the final theorem of this section.

Theorem 4.9. *Let k be a pretzel knot $P(p, q, -r)$ where p, q and r are odd numbers greater than 1. Then k has an ICON surface F in its exterior with disconnected boundary if and only if*

$$\frac{1}{p-1} + \frac{1}{q-1} = \frac{1}{r-1} \quad \textit{and} \tag{14}$$

$$\frac{g.c.d(p-1, q-1)}{g.c.d(p-1, q-1, r-1)} \quad \textit{is odd} \tag{15}$$

Moreover, the quotient (15) *is the number of boundary components of F.*

Proof. From Proposition 4.7 the integers p, q and r must satisfy identity (14). And by Lemma 4.8 there are integers u, v and g such that g.c.d$(u, v) = 1$ and:

$$\begin{aligned} p - 1 &= gu(u + v) \\ q - 1 &= gv(u + v) \\ r - 1 &= guv \end{aligned} \tag{16}$$

Then, it is not hard to see that the quotient (15) is equal to $u + v$. Now we will prove that $u + v$ is a divisor of the number of sheets m and as consequence $u + v$ will be odd. Later we will show that $m = u + v$.

First notice that the solution of $\gamma_p(x) + \gamma_q(x) + \gamma_{-r}(x) = 0$ is $x_0 = (r - 1)/r$. We can easily verify that the points $\frac{v}{u+v}\langle 1/p\rangle + \frac{u}{u+v}\langle 0/1\rangle$ and $\frac{u}{u+v}\langle 1/q\rangle + \frac{v}{u+v}\langle 0/1\rangle$ have x_0 as x coordinate. So, the number of sheets m must satisfy that the fractions $mv/(u + v)$ and $mu/(u + v)$ are integers. This means that $u + v$ is a divisor of m, as we wanted to prove.

We have proved necessity; to prove sufficiency we need to show that a pretzel knot $k = P(p, q, -r)$ with the conditions requested, has an ICON surface in its exterior. Moreover, we will show that the surface has as many boundary components as the quotient (15).

Let γ_p, γ_q and γ_{-r} be as before; that is, γ_p start at $\langle 1/p\rangle$ and ends at $\frac{v}{u+v}\langle 1/p\rangle + \frac{u}{u+v}\langle 0/1\rangle$; γ_q start at $\langle 1/q\rangle$ and ends at $\frac{u}{u+v}\langle 1/q\rangle + \frac{v}{u+v}\langle 0/1\rangle$; γ_{-r} is the constant edgepath on the vertex $\langle -1/r\rangle$. Here, we are considering u and v (and also g) the integers from lemma 4.8. The twist of this surface is 2

One thing to notice, is that g has to be an even integer. To see this, recall that p, q and r are odd numbers. Then, from equations (16) all the integers $gu(u + v)$, $gv(u + v)$ and guv have to be even, but by condition (15) $u + v$ has to be odd. So, one of the expressions $u(u + v)$ or $v(u + v)$ has to be odd, implying that g must be even.

By Proposition 2.1 in [**?**], the candidate surfaces associated to the edgepath system γ_p, γ_q and γ_{-r} are incompressible. And also, its slope would be zero. So, we only need to determine if one of the candidate surfaces is orientable with more than one odd number of sheets.

Now, let m be a possible number of sheets. As we know, m must be a multiple of $u+v$; let k be the integer such that $m = k(u+v)$. Now, we can write the endpoints of each edgepath in homogeneous coordinates:

$$\begin{aligned}\mathrm{End}(\gamma_p) &= (m, muvg, kv)\\ \mathrm{End}(\gamma_q) &= (m, muvg, ku)\\ \mathrm{End}(\gamma_{-r}) &= (m, muvg, -m)\end{aligned}$$

So, the diagrams of orientations for γ_p and γ_q are the ones shown on Fig. 25. Here, w_p, a_p, z_p, b_p and c_p are weights of lengths kv, ku, kv, $muvg$ and $muvg$, respectively; analogously w_q, a_q, z_q, b_q and c_q are weights of lengths ku, kv, ku, $muvg$ and $muvg$, respectively.

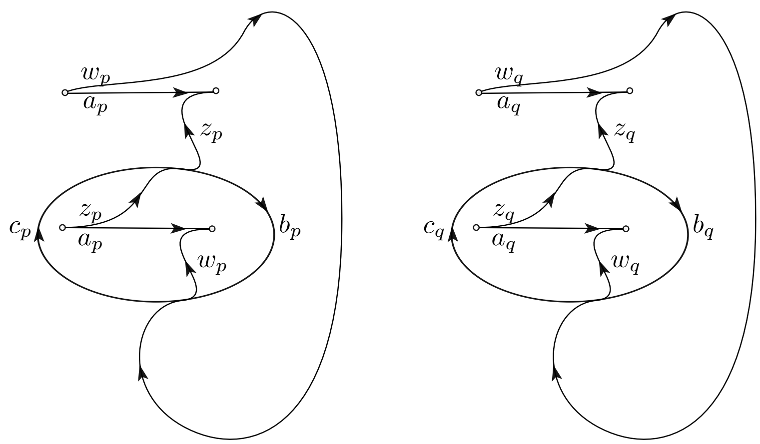

FIGURE 25. Diagram of orientation for the edgepaths γ_p and γ_q.

By the diagram of orientations, we got the relations $c_* \oplus z_* = z_* \oplus b_*$ and $b_* \oplus -J(w_*) = -J(w_*) \oplus c_*$ for $* = p, q$ (see Fig. 25). Now, we observe that:

$$b_* \oplus -J(w_*) \oplus z_* = -J(w_*) \oplus c_* \oplus z_* = -J(w_*) \oplus z_* \oplus b_* \quad \text{for } * \in \{p, q\} \tag{17}$$

That is, b_p commutes with $-J(w_p) \oplus z_p$. Also observe that $|-J(w_p) \oplus z_p| = 2kv$ divides $|b_p| = muvg$ (recall that g is even and $m = k(u+v)$), so by ([**?**], Proposition 7.1.5) we got that b_p has to be a power of $-J(w_p) \oplus z_p$. Same thing happens for c_p and $z_p \oplus -J(w_p)$.

Now, we can write b_p and c_p in terms of w_p and z_p as follows:

$$b_p = (-J(w_p) \oplus z_p)^{\frac{u(u+v)g}{2}} \qquad c_p = (z_p \oplus -J(w_p))^{\frac{u(u+v)g}{2}}$$

Similarly,

$$b_q = (-J(w_q) \oplus z_q)^{\frac{v(u+v)g}{2}} \qquad c_q = (z_q \oplus -J(w_q))^{\frac{v(u+v)g}{2}}$$

From Fig. 25 we can observe that after gluing both orientation diagrams, we will have the following relations:

$$a_p = w_q \qquad z_p = a_q \qquad a_p = z_q \qquad w_p = a_q \qquad b_p = c_q$$

These imply that $a_p = w_q = z_q$ and $a_q = w_p = z_p$. Then, we can rewrite the last relation in terms of a_p and a_q:

$$(-J(a_q) \oplus a_q)^{\frac{u(u+v)g}{2}} = b_p = c_q = (a_p \oplus -J(a_p))^{\frac{v(u+v)g}{2}}$$

By ([**?**], Proposition 7.1.6), this implies that both words $-J(a_q) \oplus a_q$ and $a_p \oplus -J(a_p)$ are powers of a smaller word s, which has length equal to the greatest common divisor of their lengths: $|-J(a_q) \oplus a_q| = 2kv$ and $|a_p \oplus -J(a_p)| = 2ku$ which is $2k$. But, since $w = -J(w)$ where $w = -J(a_q) \oplus a_q$ is a power of s, then $s = -J(s)$. So there is a word t of length k such that $s = t \oplus -J(t)$.

Summarizing, using the word t we can define the values of all the variables involved in the two diagrams of orientations in Fig. 25, and the relations resulting from gluing will be satisfied. Now, as the edgepath γ_{-r} is constant, it will not bring any new relation, so the variable t parametrizes the set of possible orientations of the candidate surface; then the candidate surface will be orientable with $|t| = k$ connected components. As we want the surface to be connected, then we need $k = 1$.

We have therefore proved that the candidate surface, in addition to being incompressible and with zero slope, is orientable and has $m = k(u+v) = u+v$ boundary components.

□

5. The Main Theorem

Lemma 5.1. *Let F be a CON (compact, orientable and non-separating) surface in the exterior E of a knot. Then, there is another surface F' ICON on E with $g(F') \leq g(F)$ and $|\partial F'| \leq |\partial F|$ such that there is an epimorphism $\pi_1(E/F') \to \pi_1(E/F)$.*

Proof. If F is incompressible there is nothing else to do. If F is compressible there is an incompressible disk for F, that is, a disk D on E such that $F \cap D = \partial D$, $\partial E \cap D = \emptyset$, and ∂D does not bound a disk on F.

Now, we have two possibilities, that ∂D separates F or not.

Case 1. $F - \partial D$ is connected. We can do surgery on F along D, and get a new surface $\widetilde{F}$ (see Fig. 26).

Let $B = D \times [0,1]$ be the cylinder containing D such that $B \cap F = \partial D \times [0,1]$ and $B \cap \widetilde{F} = D \times \{0,1\}$. Now, the natural projections $E/F \to E/(F \cup B)$ and $E/\widetilde{F} \to E/(F \cup B)$ induce two morphisms on fundamental groups; the first one is an isomorphism because $B/(B \cap F) \subset E/F$ is π_1 trivial and the second one induces an epimorphism because $\pi_1(B/(B \cap \widetilde{F})) \cong \mathbb{Z}$. So, there is an epimorphism from $\pi_1(E/\widetilde{F})$ to $\pi_1(E/F)$.

As we can recall, F is orientable and non-separating. That implies that there is an arc α over $\partial E - \partial F$ such that α touches both sides of F. Since the interior of

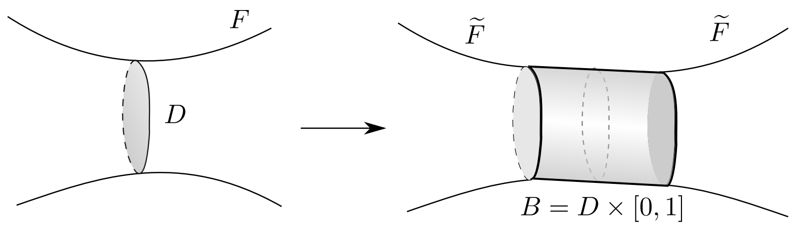

FIGURE 26. Compression of F with a disk D.

α is contained in the complement of $\widetilde{F}$, $\widetilde{F}$ will be non-separating. Then we have found a surface with the required conditions.

Case 2. $F - \partial D$ is disconnected. Let F' be the closure of the component of $F - \partial D$ with an odd number of boundary components. Now, $\widetilde{F} = F' \cup D$ is a properly embedded surface in E which is non-separating because it has slope zero, with an odd number of boundary components.

Therefore, we have the following morphisms of groups:

$$\pi_1\left(\frac{E}{F'}\right) \to \pi_1\left(\frac{E}{\widetilde{F}}\right) \tag{18}$$

$$\pi_1\left(\frac{E}{F'}\right) \to \pi_1\left(\frac{E}{F}\right) \tag{19}$$

The first morphism (18) is an isomorphism because D in the quotient E/F' is π_1 trivial. Similarly, the morphism (19) is an epimorphism because the image of $F - F'$ is a connected subset in E/F'. Therefore, there is an epimorphism from $\pi_1(E/\widetilde{F})$ to $\pi_1(E/F)$ as we want.

Summarizing, in both cases we were able to construct a surface $\widetilde{F}$ that has less genus and satisfies that there is an epimorphism $\pi_1(E/\widetilde{F}) \to \pi_1(E/F)$.

We can repeat this process repeatedly (now for $\widetilde{F}$) until we end with an incompressible surface satisfying all the conditions of the theorem. □

Definition 5.2. A knot has *Property A-ICON* if for every F ICON surface with disconnected boundary embedded in the knot exterior E, there is an arc α on ∂E connecting two different components of ∂F such that $\partial\alpha = \alpha \cap \partial F$ and $[\alpha]$ is trivial in $\pi_1(E/F)$.

Now we are going to prove that Property A-ICON is equivalent to Property $\mathbb{Z}$.

Theorem 5.3. *A knot has Property A-ICON if and only if it has Property $\mathbb{Z}$.*

Proof. To see that Property $\mathbb{Z}$ for a knot k implies Property A-ICON observe that the closure of at least one component of $\partial E - \partial F$ has a spanning arc α that is nulhomologous in E/F, because the algebraic intersection of a meridian in ∂E with ∂F is ± 1, and therefore some arc α of ∂E (that is the closure of a component of $\partial E - F$) intersects F on opposite directions. Then, if $\pi_1(E/F) = \mathbb{Z}$, α is trivial in $\pi_1(E/F)$.

Now we are going to prove that Property A-ICON implies Property $\mathbb{Z}$. We can apply the second part of the arguments on the proof of Theorem 14 in [**?**]; it proves that we can reduce the number of components of F by 2 by doing surgery on F along the annulus in ∂E containing α. The new surface F' satisfies that $\pi_1(E/F') \cong \pi_1(E/F)$. But F' can be compressible; then by Lemma 5.1 we can find another surface F'' now incompressible (ICON) with no more boundary components than F' such that there is an epimorphism $\pi_1(E/F'') \to \pi_1(E/F')$. We can iterate this process until the constructed surface has connected boundary; but for connected boundary Property $\mathbb{Z}$ is satisfied. Following back the iteration to the original surface we will end up with an epimorphism from $\mathbb{Z}$ to $\pi_1(E/F)$. Therefore $\pi_1(E/F) \cong \mathbb{Z}$.

□

Now, back to our case of interest. The following theorem establishes Property $\mathbb{Z}$ for the pretzels knots we have been discussing.

Theorem 5.4. *Let E the exterior of a pretzel knot $P(p,q,-r)$ with p, q and r odd positive integers. Then, $\pi_1(E/F) \cong \mathbb{Z}$ for all compact, orientable and non-separating surfaces F properly embedded in E.*

Proof. If one of p, q or r is equal to 1 then the pretzel $P(p,q,-r)$ would be a two-bridge knot. But two-bridge knots have rank two, that is, the fundamental group of their exteriors have rank two. But it was observed in [**?**] that Property $\mathbb{Z}$ holds for rank two knots.

From now on, we are going to consider the pretzel $k = P(p,q,-r)$ where p, q and r are greater than 1. We are going to prove that this pretzel has Property A-ICON.

Let F be an ICON surface in the exterior of k. As we have seen, if F has connected boundary then $\pi_1(E/F) \cong \mathbb{Z}$. So, the interesting case is when F has disconnected boundary.

Suppose that F has disconnected boundary; by Theorem 4.9, we may assume that p, q and r satisfy conditions (14) and (15)

Le D_1, D_2 and D_3 be the left half of the oriented train tracks defined by F on each of the three tangles $1/p$, $1/q$ and $-1/r$, respectively (see Fig. 27).

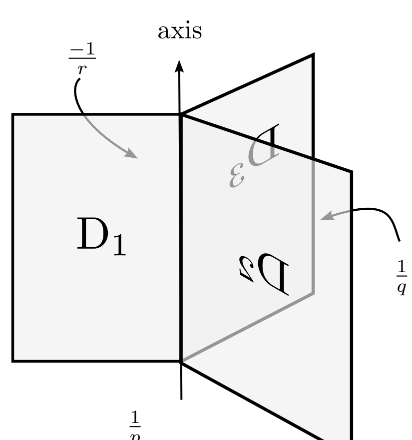

FIGURE 27. Half-planes D_1, D_2 and D_3

From the proof of Theorem 4.9 we can draw a detailed diagram for each half-plane D_i as shown in Fig. 28 where $a = ((-1)^v, (-1)^{v-1}, \ldots, (-1)^2, -1)$ and $x = ((-1)^0, (-1)^1, \ldots, (-1)^{u-1})$.

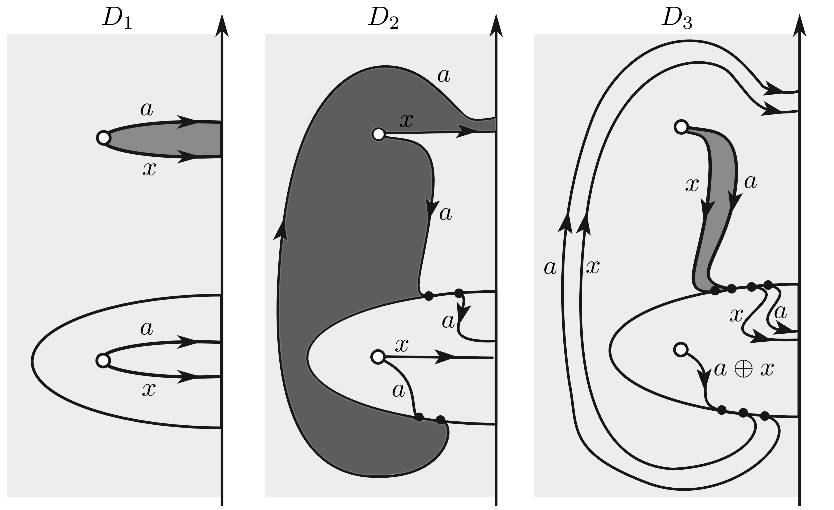

FIGURE 28. Half-planes D_1, D_2 and D_3

On Fig. 28, we highlight three regions whose union is a hexagon Ω. On the same figure, we can observe that three alternating sides of Ω are on F and the other three over ∂E.

On the upper left hole of every diagram D_i, there are two edges with weights a and x. Between those two edges, there are two arcs, one touches opposite sides of F and the other does not. The arc $\alpha_i \subset D_i$ that touches the same side of F is the one that belongs to Ω. The other arc $\beta_i \in D_i$, touches different sides of F and is the only arc properly embedded in ∂E that does that; so, all the β_i's belong to the same component of $\partial E - \partial F$. In consequence all α_i's also belong to the same component; therefore, they are isotopic in $\pi_1(E/F)$, i.e,$[\alpha_1] = [\alpha_2] = [\alpha_3]$. Moreover, $1 = [\partial\Omega] = [\alpha_1] \cdot [\alpha_2^{-1}] \cdot [\alpha_3]$ in $\pi_1(E/F)$; this implies that the arcs α_i are trivial in $\pi_1(E/F)$. □

FINAL COMMENTS

Conceivably, Conjecture $\mathbb{Z}$ can be proven, with similar techniques, for not-too-complicated Montesinos knots, perhaps those with 3 rational tangles. If we have a Montesinos knot with n rational tangles, the number of cases that have to be analyzed grows exponentially with n.

In a not-too-serious vein we think of Conjecture $\mathbb{Z}$ as a kind of inverse of the Poincaré Conjecture: in the latter, X is 1-connected and one proves X is S^3; in the former, Y is the 2-point compactification of the complement if an (I)CON surface in the exterior of a knot in S^3, and one has to prove that Y is 1-connected.

Acknowledgments

We thank Mario Eudave-Muñoz and Victor Núñez for stimulating conversations. We also thank the Reviewer for improving the presentation of the paper.